Integrated GEE-MODFLOW based Groundwater Recharge Assessment System for Hindon River System

Final Report

Funded by:

NATIONAL INSTITUTE OF HYDROLOGY, ROORKEE

DoWR, RD & GR, Ministry of Jal Shakti, Govt. of India

August 2023

PROJECT TEAM

Dr. Nitesh Patidar (PI), Scientist C

Dr. Gopal Krishan, Scientist D

Dr. Anupma Sharma, Scientist G & Head Groundwater Hydrology Division

Dr. M.K. Goel, Scientist G & Head Water Resources System Division

TABLE OF CONTENTS

LIST OF TABLES

LIST OF FIGURES

ABSTRACT

Hydrologic modelling plays a crucial role in guiding water management decisions by assessing water availability. To enhance the effectiveness of hydrologic models, a comprehensive approach integrating cloud computing, web-based interfaces, and coupled models has been developed and tested in this study. The focus lies on a web-based system designed to estimate groundwater recharge, while also simulating runoff, streamflow, evapotranspiration (ET), and crop water demand/supply using established methods. The developed system, NIH-WISDOM (NIH's **W**eb-based **I**ntegrated catchment modelling **S**ystem for **D**ecisi**o**n **M**aking), has been evaluated in the Hindon and upper Mahanadi River basins.

The key component of the integrated model comprises three modules: Root Zone Flow (RZF), Unsaturated Zone Flow (UZF), and Groundwater Flow (GWF). These modules collectively simulate processes across different hydrologic zones, from surface interactions to groundwater dynamics. RZF, developed to simulate processes in the topsoil layer (up to 500 mm depth), captures phenomena like runoff, infiltration, ET, and soil evaporation. RZF is closely linked with the UZF module, which further simulates processes in the vadose zone, including deep-root ET and recharge. The soil moisture balance leverages irrigation demand estimation in RZF. The groundwater pumping estimation is integrated based on irrigation demand. Surface Flow Routing (SFR) package of MODFLOW is employed for runoff routing to basin outlets. The UZF module simulates flow in the unsaturated zone above the water table, and it interfaces with GWF, which employs the popular MODFLOW software for groundwater flow simulation.

NIH-WISDOM extends its capabilities with the integration of Google Earth Engine (GEE) for data retrieval and processing. A user-friendly web-based interface facilitates model execution, while also enabling visualization of thematic, time-series, and 3D data. The system boasts several improvements over traditional models, including the incorporation of phenological variations using 4-day composite Leaf Area Index, automated data retrieval and processing, and the ability to disseminate outputs on web-based platforms to aid decision-making.

Results showcase the model's performance through comparisons of observed groundwater head with the simulated heads at different locations. The model domain for Hindon is extended up to river Yamuna in the West and river Ganga in the East to appropriately assign the boundary conditions and the extended domain is called Ganga-Yamuna Doab (GYD). A satisfactory performance is observed with R^2 of 0.98, 0.62, 0.74 and 0.87 during 2011, 2013, 2015 and 2018, respectively. It is found that the spatial pattern is reasonably captured by model implies that the results are useful for assessing spatial patterns at seasonal and annual scales. The Root Mean Square Error (RMSE) varies considerably at each observation well indicating spatially inconstant model performance. It is observed that the simulated heads deviate severely from the observed heads at some locations (such as *Lakhaothi*), specially during the later period (say after 2015). These discrepancies indicates that the model outputs with currently available data sets does not provide reliable results at daily/monthly time-steps, although, the results at annual scale and the spatial maps could still be useful for various impact assessments. The district-wise recharge estimates of CGWB for the year 2012 and 2016 are compared with model outputs in GYD. The simulated recharge reasonably matches with CGWB's assessments. A high

difference in recharge is observed for some districts, such as *Meerut* and *Baghpat*. It is also seen that the recharge matches more closely for the year 2012 as compared to 2016. The simulated streamflow is compared with the observed streamflow at Basantpur in upper Mahanadi basin. The model satisfactorily simulates streamflow at monthly time-scale with Nash-sutcliffe Efficiency (NSE) of 0.6. It is found that for the year of normal precipitation, such as 2003 and 2005, the simulation of peak flows is better than that is in the higher or lower precipitation years, such as 2001 and 2002.

The scenario analysis investigates the impact of altered groundwater recharge and pumping scenarios on groundwater levels. The scenarios of groundwater recharge and extraction were formulated by perturbing the Business-as-Usual (BAU) recharge and extractions. Three scenarios of increased recharge, by 10, 20 and 30%, were prepared. Similarly, two scenarios of increased groundwater extraction by 20 and 40% were prepared. In the GYD, the average annual recharge to groundwater is estimated as 312 mm under BAU scenario. The recharge is increased to 343.2, 374.4 and 405.6 mm under scenarios of 10, 20 and 30% increased recharge, respectively. Under BAU Scenario, depth to groundwater is shallow near the rivers and towards the North-eastern parts. A patch of deep groundwater is observed in the centre towards West with depth up to ~25 m. Under the scenarios of increased recharge, a considerable improvement in depth to groundwater is observed. The aquifer starts recovery when recharge is increased by 10%. With 20% increase in recharge, a considerable improvement in the groundwater levels is observed and the areas of overexploited groundwater improves considerably. Under the scenarios of 30% increase in recharge, the depleted groundwater recovers completely, however, in the areas of shallow groundwater, the groundwater rises near the ground surface which might lead to water-logging in these areas. It is found that managed recharge scenarios, particularly a 20% increase in recharge, could contribute to improved groundwater sustainability, indicating potential benefits for water resource planning.

The average annual groundwater extraction is estimated as 9,557 MCM under BAU scenario in GYD. The extraction is increased to 11,469 and 13,033 MCM under the increased extraction by 20% and 40%, respectively. The aquifer starts depleting when pumping is increased by 20%. With 40% increase in pumping, a considerable depletion in groundwater is expected and the central area becomes overexploited with depth to groundwater up to 45 m. The analysis indicates that if such increase in pumping occurs, the groundwater system of GYD might fail to supply water in many parts of the basin. In addition, such increase in pumping might lead to poor groundwater quality and reduced baseflow contribution to rives.

The study acknowledges certain limitations, such as the need for improved data quality and availability, tuning of algorithmic thresholds, and the requirement for improved computation efficiency. The need for further enhancement is recognized, including incorporating surface hydrologic models like the Variable Infiltration Capacity (VIC) model, refining hydraulic connections algorithm for SFR, and offering options for independent model runs.

In conclusion, the study introduces NIH-WISDOM as an integrated hydrologic modelling system that combines cloud computing, web-based interfaces, and established modelling techniques to estimate groundwater recharge and related processes. The system's performance,

strengths, limitations, and avenues for future improvements have been comprehensively discussed in this report.

Chapter-1

INTRODUCTION

1.1 Background

Groundwater resource has a significant contribution to meet societal needs and development objectives in India. In many parts of the country, groundwater is often the sole source of water and thus plays an important role in socioeconomic development of the country. However, the excessive groundwater withdrawal led by growing water demands has imposed additional pressure on groundwater resources which has resulted in rapid and widespread groundwater declines. An assessment of country's groundwater by Central Groundwater Board (CGWB) reveals that out of the total 7089 blocks of the country, 14% are over-exploited, 4% are critical and 12% are semi-critical (CGWB, 2022). Further, the declining groundwater levels due to over-exploitation has raised several queries about the changes in river water availability due to adverse impacts of aquifer depletion, vulnerability of groundwater contamination, and availability of surface and subsurface water resources in the future (Mukherjee et al., 2018; Voss et al., 2013). Therefore, to answer these queries and manage water resources in a sustainable manner, comprehensive understanding of groundwater system is essential. Of particular importance are the understanding of recharge processes, quantification of recharge from various sources, such as rainfall and surface water bodies, assessment of the impacts of groundwater withdrawal, and understanding of exchange of fluxes between the surface and subsurface hydrological systems.

Groundwater recharge estimation has gained prime importance during the recent years due to increasing focus on groundwater management (Abiye, 2016; Assefa & Woodbury, 2013; Mountjoy Daniel & Low Glen, 2017; Szabó et al., 2023). Recently, several measures have been initiated by Government agencies to reduce over-exploitation and recover depleted aquifers of the country (CGWB, 2020). In this context, the Manages Aquifer Recharge (MAR) and river rejuvenation have been the key focus of the Government for ensuring future water availability. However, with limited hydrologic observations, such as groundwater levels, recharge and baseflow, implementation of MAR and rejuvenation projects would be difficult. Moreover, implementation of such projects would require estimates of current state of surface and groundwater resources, identification of suitable measures, assessment of possible implications of the projects and future prediction of water demand and supply for sustainable management (Alam et al., 2021; Imig et al., 2022; Zhang et al., 2020). Therefore, a holistic approach that includes various models, observations, decision support tools and expert knowledge would be required.

1.2 Integrated modelling for surface-groundwater flow simulation

Groundwater recharge can be considered as a link between surface and groundwater fluxes. The water that infiltrates to the soil transits through vadose zone to join groundwater and water that reaches to groundwater is called recharge. To estimate groundwater recharge, simulation

of both the surface and subsurface processes is required (Cao et al., 2016; Zomlot et al., 2015). Infiltration is governed by various surface processes, including runoff, soil moisture, ET, etc. The unsaturated flow through vadose zone depends upon root water uptake by plants, soil moisture conditions and soil hydraulic forces (Niswonger et al., 2006). The thickness of vadose zone depends upon the groundwater level. These close interactions between surface-subsurface processes necessitates simulation of all processes in an integrated manner for reliable estimates of recharge. In addition, due to difficulties in the direct measurement of recharge, the validation of recharge is generally performed indirectly using groundwater fluctuations and infiltration rates (Scanlon et al., 2002). Therefore, application of a model, that simulates surface hydrological processes only, may not be very useful for recharge estimation. However, such applications of independent surface hydrologic models are widely available in literature. Probably, the high computation burden, huge data requirement and complex model configuration of integrated models led to limited applications of integrated models for recharge estimation during the past decades.

Numerous integrated hydrologic models have been developed. The selection of models and their integration depends on the purpose of integrated modelling. For simulation of hydrologic fluxes, such as runoff, recharge, streamflow and groundwater levels, integration of surface-groundwater model is appropriate(Bailey et al., 2016a). To simulate water demand and supply along with surface and groundwater availability, a system model with irrigation module would be required. Similarly, an integrated eco-hydrologic model would be required for simulating linkages between ecology and hydrology(Boulain et al., 2009; Peng et al., 2015). Several integrated models have been developed, such as SWAT-MODFLOW, VIC-MODFLOW, GSFLOW, WetSpass-MODFLOW and WEAP. The SWAT-MODFLOW is an integration of popular Soil and Water Assessment Tool (SWAT) and groundwater flow model MODFLOW (Bailey et al., 2016b; Neitsch et al., 2011). It can simulate all surface-subsurface hydrologic components and particularly useful for simulating recharge, baseflow and streamflow. The VIC-MODFLOW is an integration of macro-scale grid-based model Variable Infiltration Capacity (VIC) model and MODFLOW which is developed to simulate unsaturated flow and along with other surface-subsurface processes for large scale applications (Bay et al., 2019). GSFLOW is an integration of Precipitation-runoff Modelling system (PRMS) and MODFLOW which is improve simulation of baseflow. The WetSpass-MODFLOW is developed to simulate groundwater recharge and asses responses of recharge to groundwater system at monthly/seasonal scale (Batelaan & DeSmedt, 2001). WEAP aims at simulating crop water requirement and supply from surface and groundwater utilizing integrated approach (Constance L Danner et al., 2006).

1.3 MODFLOW

MODFLOW is modular program developed by USGS. It is the most popular program for groundwater flow and transport modelling and has been widely used with other models for integrated simulation. Development of MODFLOW started in 1980's with its first version launched in 1983. Initially, the MODFLOW consists of modules for groundwater flow simulation, which has expanded now to a more comprehensive model. In addition to its capabilities in simulating groundwater flow and transport, it also encompasses various other

modules that allow easy coupling with other models(Langevin et al., 2017). Important modules for coupling include Unsaturated Zone Flow (UZF), Surface Flow Routing (SFR), Evapotranspiration (ET) and Recharge (RCH). The ET and RCH packages can take input in the form of potential evapotranspiration and percolation, respectively, which are generally simulated using surface hydrologic models. The UZF simulates the movement of moisture in vadose zone, plant water uptake and recharge. The UZF also needs various influxes which can be simulated using surface hydrologic models. The SFR is an important module for baseflow simulation which can utilize surface runoff and diversions from rivers as simulated by surface hydrologic models and route them to the catchment outlet. In addition, the modular structure of MODFLOW makes it compatible with other surface hydrologic models and therefore it has been widely used as groundwater model for integrated hydrologic simulation.

1.4 Google Earth Engine

Google Earth Engine (GEE) – a cloud-based platform developed by Google – is powerful tool that encompasses various spatial data and allows on-cloud geospatial processing utilizing high-performance computing infrastructure of Google (Gorelick et al., 2017; Mutanga & Kumar, 2019; Vos et al., 2019; Yang et al., 2022). Petabytes of spatial data for various remote sensing applications are ingested into GEE which can be processed on GEE itself utilizing Java-script and Python Application Programming Interfaces (APIs). Several derived products, such as precipitation, potential evapotranspiration and Leaf Area Index (LAI) are shared by various researchers and agencies for further utilization for modelling and analysis. With its powerful on-cloud data processing APIs, the GEE is an appropriate tool for automated data processing for hydrologic modelling. Various GEE-based tools have been developed recently for various applications.

1.5 Web-based systems

Desktop-based hydrologic models have been helping the modellers since more than three decades. With advanced computing hardware and modern interface layout, such desktop-based models have become fast and easy-to-use. In the recent years, the web-based systems have gained popularity. The web-based systems have several advantages, such as:

I. It does not require expensive hardware in user computer as the heavy computations are performed on server.
II. It does not require any configuration in user computer and can be run simply using a web browser.
III. Allows automation and use of pre-processed data on server. This also eliminates the need of storing data on user computer.

Although desktop-based models produce reliable hydrologic simulations these still consume considerable time, particularly in downloading and processing time-series and spatial data. In addition, these do not allow dissemination of model outputs through web which can be done efficiently using web-based systems. The desktop-based models have several advantages as well, such as, it provides more control and options for data manipulation and model tuning, and better options to modify model source codes for incorporating new processes. Recently, use of web-based applications has increased substantially due to their ease of accessibility and easy-to-use interactive interface. Sallwey et al. (2019) has developed a web-based tool for site

suitability mapping using MCDA. Use of high-performance computing systems and cloud-computing infrastructures have empowered web-applications considerably in recent decade (Evans et al., 2020; White et al., 2021). Unfortunately, integrated use of these state-of-the-art tools and techniques still requires considerable expertise and skills in modelling, spatial data processing, Information Technology (IT), programming, cloud computing and web-development.

With the improved understanding of hydrological processes and recent advancements in the field of computers, many hydrological models have been developed. Although the models developed during the past decades produce useful results, a model alone may not be implemented to support decision making for groundwater management mainly due to (i) difficulties in incorporating the frequent changes in impervious surface, vegetation phenology and surface water bodies, and (ii) no provision to disseminate the outputs to open platforms so as to support decision making. Therefore, a Groundwater Recharge Assessment System, that integrates state-of-the-art hydrological models, allows to incorporate frequently available remote sensing data, data visualization and dissemination, is required for precise estimation of groundwater recharge and to support decision making in India.

1.6 Objectives

I. Development of the integrated GEE-MODFLOW model to estimate groundwater recharge and to disseminate model outputs.
II. Application of the integrated GEE-MODFLOW model in Hindon and upper Mahanadi River basins.
III. Application of the integrated GEE-MODFLOW model to assess the impacts of various recharge/abstraction scenarios on groundwater system of Hindon river basin.

***

Chapter-2

DEVELOPMENT OF SYSTEM FOR INTEGRATED MODELLING

Groundwater recharge is an end-result of various processes happening in surface-subsurface and governed by various influxes, such infiltration and irrigation, and outfluxes, such as root water uptake and soil evaporation. Therefore, in order to mimic all such processes, an integrated model is needed. The integrated model developed in this study consists of various modules which simulate processes in unsaturated and saturated zones. The model has three simulation modules, namely Root Zone Flow (RZF), Unsaturated Zone Flow (UZF), and Groundwater Flow (GWF) (Figure 2.1). The integrated model is encapsulated into a web-based system which consists of python-based modules, Google Earth Engine (GEE) API, thematic and time-series database. The developed integrated system is named as NIH's Web-based Integrated Catchment Modelling System for Decision Making (NIH-WISDOM). It is empowered by well-stablished hydrologic models, such as MODFLOW, for reliable hydrologic simulations. Theory and concepts used in the integrated model are elaborated below.

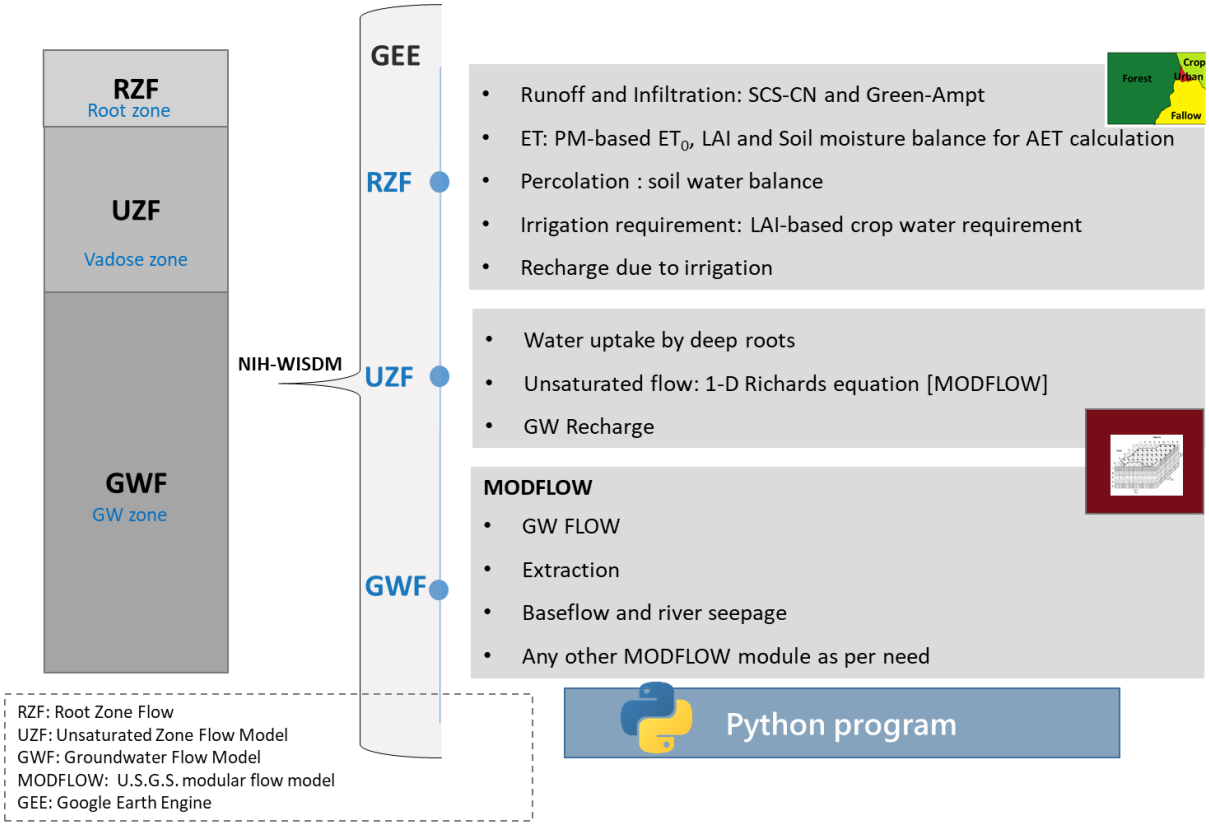

Figure 2.1. Methods used in simulating surface and sub-surface hydrological variables

2.1 Root Zone Flow (RZF) Module

The RZF is developed during the present study at NIH to simulate processes in the top soil layer (say, upto 500 mm). All the processes happening at top soil layer, such as runoff,

infiltration, ET from top soil layer, soil evaporation, etc., are simulated by RZF. RZF is tightly coupled with Unsaturated Zone Flow (UZF) module to further simulate the processes in the vadose zone, such as ET from deep roots and recharge. RZF uses the well-established methods of hydrology to simulate various components, such as SCS-CN, Green-Ampt, Penman-Monteith, etc. These methods are elaborated in the following sections.

2.1.1 Runoff and infiltration

The model provides two methods for estimating runoff, the SCS-CN and Green-Ampt. Runoff is simulated using Green-Ampt when the sub-daily precipitation data is available, the SCS-CN is used otherwise.

SCS-CN method

The Soil Conservation Service - Curve Number (SCS - CN) method is developed by Soil Conservation Service (now called the Natural Resources Conservation Service), U.S. Department of Agriculture (USDA - SCS, 1972). Since its introduction in 1954, the SCS-CN method has become the standard method, in practice, for estimating an event-based rainfall-runoff response. In addition, the popular models, such as Soil and Water Assessment Tool (SWAT) and Soil Water Balance (SWB) Model of USGS, use it for runoff simulation at daily time-step.

According to the SCS-CN method, the ratio of the actual amount of direct runoff to the maximum potential runoff is equal to the ratio of the amount of actual infiltration to the amount of the potential maximum retention. It also assumes that the initial abstractions are fraction of the maximum potential retention. The runoff can be estimated using Eq-2.1.

$$Q = \frac{(P-I_a)^2}{(P-I_a+S)} \tag{2.1}$$

Where, Q is the direct runoff, P is precipitation, I_a is initial abstraction and S is the maximum potential retention. Generally, the I_a is considered as 20% of S, however, in some cases it varies with precipitation intensity. The S is estimated using the Curve Number which is assigned based on combination of land uses and soil.

$$S = \frac{25400}{CN} - 254 \tag{2.2}$$

Where, S is in mm. The CN is assigned using standard values available from literature considering the land uses and soil hydrologic group. Once the runoff is derived, infiltration can be derived using water balance. Total infiltration (F_{day}) at a grid can be estimated as

$$F_{day} = F_i + F_u \tag{2.3}$$

where,

$$F_i = 0.2 \times S - i \quad \textit{for } i \leq 0.2 \times S \tag{2.4}$$

$$F_i = 0 \quad \textit{for } i > 0.2 \times S \tag{2.5}$$

$$F_u = P - 0.2 \times S - R \quad \textit{for } P \geq 0.2 \times S - P \tag{2.6}$$

$$F_u = 0 \quad \textit{for } P < 0.2 \times S - P \tag{2.7}$$

Where, i is interception, F_i is initial infiltration and F_u is final infiltration.

2.1.2 Modifications to SCS-CN

In standard application of SCS-CN method, the condition of land use is generally ignored and the CN values are assigned assuming average/good condition. However, in real, the classes such as forest/shrubs exhibits considerable variations in canopy coverage which affects the canopy interception. In addition, considering rapid urbanization, the impervious surface cannot be assumed constant for entire simulation period. Generally, the CN of urban areas are assigned taking a single land use map which might introduce uncertainties in the runoff estimation as there might have several land cover changes during the period of simulation. In the developed model, the CN is assigned dynamically considering the canopy coverage (8-daily) and impervious surface (annual) time series data. The CN values are assigned at each time step by interpolating values between a user specified minimum and maximum CN values.

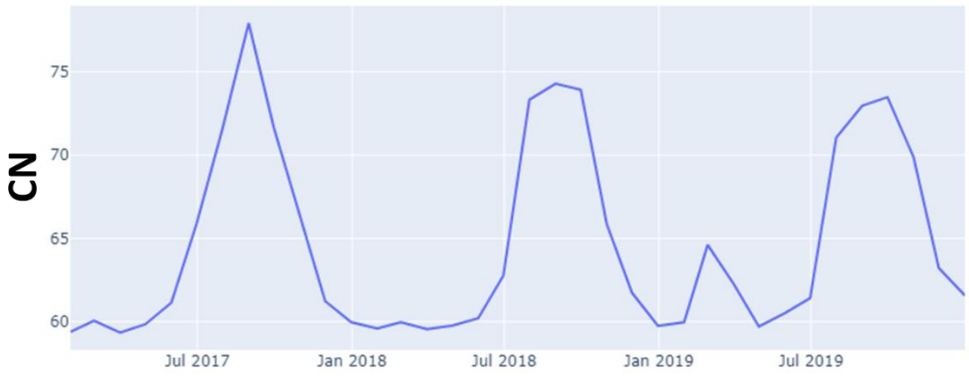

Figure 2.2. CN values in a forest grid using the developed approach

2.1.3 Green-Ampt (GA) method

The GA method is developed by Green and Ampt in 1911 by applying Darcy's law to homogeneous soil with constant hydraulic conductivity, initial water content and head at the wetting front. They proposed a simple model for water infiltration into a homogeneous soil with a uniform initial water content. The saturated wetting front is assumed to move downwards as a single piston like displacement.

The GA is a process-based model which can simulate sub-daily infiltration. It simulates instant infiltration rate for a given wetting front. The location of wetting front is updated after each iteration. The cumulative infiltration can also be simulated using the GA method. The infiltration rate at a given time is given by the following equation.

$$f(t) = K_s + K_s \frac{|\psi_f|(\theta_s - \theta_i)}{F} \qquad for\ t > t_p \qquad (2.8)$$

$$f(t) = P \qquad for\ t \leq t_p \qquad (2.9)$$

Where, f(t) indicates rate of infiltration (L/T), K_s is the saturated hydraulic conductivity, ψ_f is the matric potential at the wetting front, θ_i and θ_s are the initial and saturated soil moisture contents, and F is the cumulative infiltration (L). In order to estimate f(t), the time to ponding is to be estimated first using the following equation.

$$t = t_p + \frac{1}{K_s}\left[F - F_p + |\psi_f|(\theta_s - \theta_i)\ln\left(\frac{|\psi_f|(\theta_s-\theta_i)+F_p}{|\psi_f|(\theta_s-\theta_i)+F}\right)\right] \quad (2.10)$$

where F_p is the amount of water that infiltrates before water begins to pond at the surface and t_p is the time it takes to have water begin to pond at the surface [T]. The F_p *and* t_p can be estimated using the expression:

$$F_p = \frac{|\psi_f|K_s(\theta_s-\theta_i)}{P-K_s} \qquad t=t_p \text{ and } P>K_s \quad (2.11)$$

$$t_p = \frac{F_p}{P} \quad (2.12)$$

Equation 2.11 is solved for F_p in the model using the Newton-Raphson method. The θ_i is updated at daily time step. The daily cumulative infiltration is then used in the other water balance calculations. In GA method, the infiltration is estimated first, the runoff is then estimated using the water balance approach. The interception losses and infiltration are subtracted from the total precipitation to get the runoff. Since the GA is applied at sub-daily time step, the daily runoff is estimated by summing the runoff for the respective day.

2.1.3 Evapotranspiration (ET)

Potential Evapotranspiration (PET) is estimated using Penman-Monteith equation. The Actual ET (AET) is then estimated by applying the vegetation and soil moisture resistances over PET. The model divides the grid cell into three biophysical components, i.e. vegetation, soil and impervious surface for estimating the AET. The maximum transpiration from the vegetated fraction is estimated using the empirical relationship between maximum transpiration and Leaf Area Index (LAI) as follows:

$$Tr_{max} = PET \times (LAI/3) \qquad for\ LAI \leq 3 \quad (2.13)$$

$$Tr_{max} = PET \qquad for\ LAI > 3 \quad (2.14)$$

Where, Tr_{max} is the maximum transpiration from the vegetation. The water uptake from the roots varies with depth, it is found that a major portion of transpiration occurs from the top soil layer. According to FAO, 40% of the total transpiration occurs from just 25% of root depth. To simulate this phenomenon, the following exponential relationship is used. The same is also employed in the well-known hydrological model-SWAT. This decay of transpiration with depth is estimated essentially to divide the ET from top and bottom soil layers. The maximum transpiration from the top soil layer ($tr_{max\text{-}top}$) is estimated as

$$Tr_{max-top} = Tr_{max} \times \frac{\left(1-e^{-\beta \times depth/root\_depth}\right)}{\left(1-e^{-\beta}\right)} \quad (2.15)$$

Where, *depth* indicates soil layer depth, *root_depth* indicates the root depth of the vegetation. The maximum transpiration from the bottom soil is estimated by subtracting the $Tr_{max-top}$ from Tr_{max}. Further, to estimate the actual transpiration the soil moisture availability constraint is imposed. Actual transpiration from the top soil layer is estimated as

$$ATr_{top} = Tr_{max-top} \qquad \text{for AMC} \geq 0.25 \times AMC_{max} \quad (2.16)$$

$$ATr_{top} = Tr_{max-top} \times e^{(5\times\left(\frac{AMC}{(0.25\times AMC_{max})}\right)-1)} \quad \text{for AMC} < 0.25\times\text{AMC}_{max} \quad (2.17)$$

Where, AMC_{max} is the maximum available soil moisture and AMC is the available soil moisture at the respective time step. In order to check if the actual transpiration is not exceeding the AMC, the minimum of the ATr_{top} and ($depth\times AMC$) is taken as the final ATr_{top}. The soil evaporation also decreases exponentially with depth. The evaporation from the top soil layer is estimated using the following relationship.

$$Ev_{max} = PET \times SCI \quad (2.18)$$

$$Ev_{\max\_top} = Ev_{max} \times \left(\frac{depth}{(depth + e^{(2.374-0.00713\times depth)})}\right) \quad (2.19)$$

Where, Ev_{max} is the maximum soil evaporation, SCI is Soil Cover Index, Ev_{max_top} is the maximum soil evaporation from the top soil. The actual soil evaporation from the top soil is estimated by constraining the maximum evaporation by the available soil moisture in the soil layer. The actual evaporation from the top soil AEv_{top} can be estimated using the following equation.

$$AEv_{top} = Ev_{top} \times e^{\left(2.5\times\frac{(\theta-FC)}{(FC-WP)}\right)} \quad for\ \theta < FC \quad (2.20)$$

$$AEv_{top} = Ev_{top} \quad \text{for } \theta \geq FC \quad (2.21)$$

Where, θ is the soil moisture at the time step, FC is the field capacity and WP is the wilting point. Further, it the maximum actual evaporation from the soil is restricted to a maximum of 80% of total available soil moisture in the layer on the respective time step. The actual total ET is the sum of transpiration and soil evaporation weighted by the fractions of vegetation and soil within the soil grid.

2.1.4 Soil moisture in top soil layer

Change in soil moisture is estimated at each time step by performing soil moisture balance. If soil moisture exceeds the maximum moisture holding capacity of the soil, the excess soil moisture content is converted to depth from volumetric water content and is considered as percolation to the second layer. At every time-step, change in soil moisture storage (Δθ) is calculated using the following formula.

$$\Delta\theta = \theta_{i-1} - AET_i + FIR_i \quad (2.22)$$

Where, θ_{i-1} is soil moisture during previous time-step, AET is actual ET, FIR is field irrigation requirement, and i represent the time-step. Once the change in soil moisture is estimated, the soil moisture at the end of the time-step i is estimated as:

$$\theta_i = \theta_{i-1} + \Delta\theta \times depth \quad (2.23)$$

where, *depth* indicates soil layer depth.

2.1.5 Irrigation demand and supply

Irrigation is an important influx to sub-surface system that considerably affects AET, soil moisture and recharge. To make the recharge estimation more realistic, the inclusion of irrigation is therefore important. Estimation of irrigation demand in the model is based on the soil moisture balance in the RZF. At each time-step, the available soil moisture is estimated and the irrigation is added when soil moisture depletes beyond the specified allowable depletion.

$$FIR_i = (FC - \theta_i) \times root\_depth \times vegFrac / (\eta_{app}/100) \quad (2.24)$$

Where, vegFrac is the fraction of vegetation in the model grid, and η_{app} is irrigation application efficiency (%). Note that the FIR is only estimated at time-steps when the soil moisture depletes below allowable limits. Effect of irrigation is simultaneously considered by supplying the amount of required irrigation (FIR). Change in soil moisture due to irrigation is considered using the equations 2.22 and 2.23.

2.1.6 Groundwater extraction

Groundwater pumping is an important component to estimate safe groundwater extraction and is also an input to MODFLOW. The rates of groundwater extractions are not readily available for most of the regions in India. Generally, such data are estimated using electricity bills assuming that the power consumptions is mainly due to groundwater pumps used in the agricultural fields. Other approach is to estimate such data using crop water requirement or groundwater fluctuations. However, despite considerable efforts by various government departments, it is still difficult to obtain time-series (say, monthly) of pumping using such methods which is a vital input to modelling. In the developed model, groundwater extractions are estimated internally utilizing the irrigation demand estimates. Since irrigation in many regions is applied from surface water (canal, tanks, lakes, etc.), it is important to subtract the demand that met from surface water. To incorporate this, fraction of demand that is met from surface water is to be supplied to model. The remaining demand is then met from groundwater. The model automatically generates pumping requirements under each grid and generates required mudflow files for well package.

2.1.7 Routing of runoff

For estimation of baseflow/river seepage and calibration/validation of integrated model, it is important to rout the runoff to the basin outlet / discharge gauging sites. The routing models require various inputs related to river geometry, segment lengths and hydraulic connectivity between reaches. Also, to route the overland flow to river, it is important to know watershed of each river reach and their connectivity. Creation of such inputs require considerable effort and time. In the developed model, derivation of these river attributes is automated utilizing HydroShed (Lehner et al., 2008) and Global River Database (Andreadis et al., 2013). Runoff routing is done using the Surface Flow Routing (SFR) package of MODFLOW. The module also requires various inputs related to river hydraulic connectivity and riverbed thickness in addition to the river attributes mentioned above. Input preparation for SFR is a complex task as it requires grid-wise river reach connections along with parameters. For instance, connection

of each grid to its upstream and downstream grids should be mentioned and derivation of which may not be straightforward.

The developed model uses an algorithm to derive grid-wise inputs for SFR utilizing HydroSheds river and catchment layers. The algorithm transforms the river segment-level data to grid-level using various decision rules which compares elevation of target grid to neighboring grids, ensures continuous flow between grids, and logically verifies the grid connections.

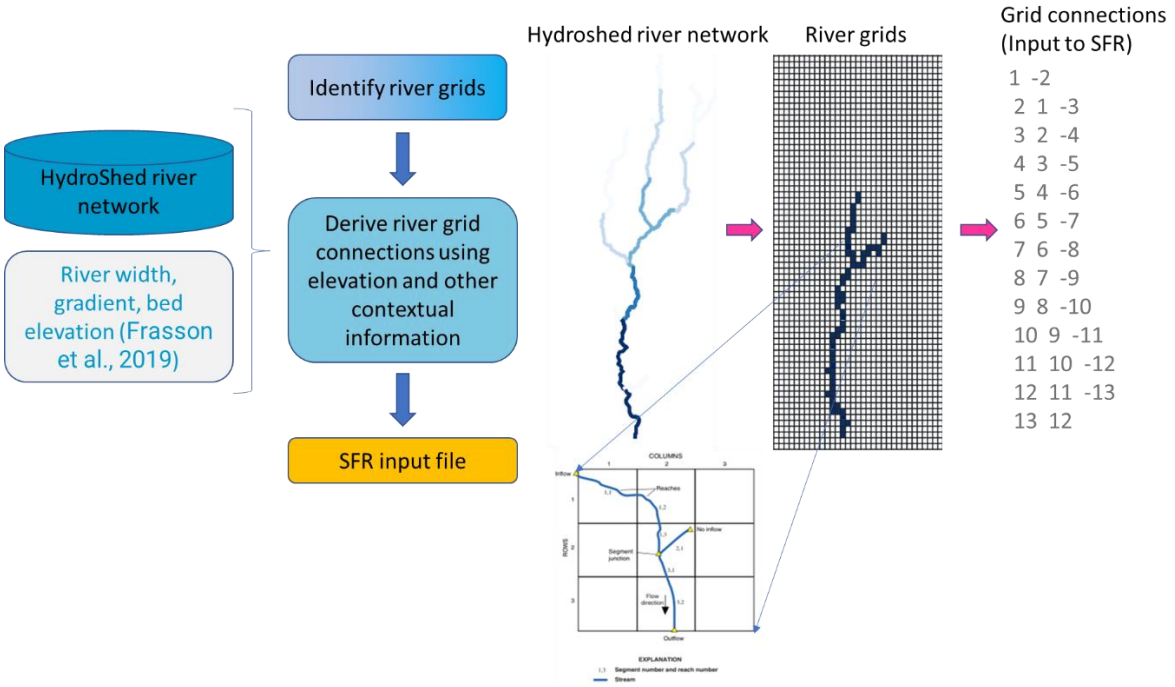

Figure 2.3. Schematic of workflow in river routing algorithm of WISDOM

Streamflow routing within the SFR Package is based on the continuity equation and assumption of piecewise steady (nonchanging in discrete time periods), uniform (nonchanging in location), and constant-density streamflow, such that during all times, volumetric inflow and outflow rates are equal and no water is added to or removed from storage in the surface channels. Flow between streams and aquifers in the groundwater model is computed using Darcy's Law and assuming uniform flow between a stream and aquifer over a given section of stream and corresponding volume of aquifer. This flow is computed as:

$$Q_{sw-gw} = \frac{KwL}{m}(h_s - h_a) \tag{2.25}$$

Where, Q_{sw-gw} is volumetric exchange between river and groundwater, K is river hydraulic conductivity, w is width of river, L is Length of river segment, m is riverbed thickness, h_s is river stage, and h_a is groundwater head. Assuming a wide rectangular stream channel in which the stream width is much greater than the stream depth, Manning's equation is applied in SFR to estimate river stage. Detailed description of the concepts and theory used in SFR can be found in SFR documentation (Niswonger & Prudic, 2010).

2.2 Unsaturated Zone Flow (UZF) Module

UZF aims at simulating the flow in unsaturated zone. In case of WISDOM, the UZF simulates flow in the zone below the root zone (as simulated by RZF) but above the water table. UZF is a 1-D Richards Equation-based module of MODFLOW which is tightly coupled with RZF and GWF modules. The percolation from the top soil layer becomes the influx to the bottom soil layer which consists the deeper root and the unsaturated zone. The moisture movement in the unsaturated zone is simulated at daily time-step. The actual transpiration from the deep roots is also estimated by UZF. Maximum transpiration from deep root as estimated by subtracting the actual transpiration occurred at the top soil layer from the maximum transpiration, becomes input to UZF. In UZF, the actual transpiration from the deeper roots is estimated considering the moisture availability at each time-step. Finally, the sum of transpiration from the top and bottom soil layers is summed to get the total transpiration. The 1-D Richards equation represents the movement of water in unsaturated soil using a nonlinear partial differential equation

$$\frac{\partial \theta}{\partial t} = \frac{\partial q}{\partial z} - i = \frac{\partial}{\partial z}\left[D(\theta)\frac{\partial \theta}{\partial z} - K(\theta)\right] - i \tag{2.26}$$

Where, the q is the Water flux, i.e. percolation from the top soil layer, z is the elevation, D(θ) is the hydraulic diffusivity, K(θ) is unsaturated hydraulic conductivity, I indicates ET rate, I.e. the transpiration from the deep roots. The Richards equation is solved using the Finite Difference Method (FDE) in MODFLOW. Finally, the volumetric outflux, so called the recharge, is estimated. The detail description of the Richards equation and UZF is out of the scope of this report, however, it can be found in UZF documentation (Niswonger et al., 2006).

2.3 Groundwater Flow (GWF) Module

Groundwater flow simulation is vital for simulation of recharge-pumping effects and river-aquifer interaction. In addition, integration of groundwater model help validating the recharge by comparing groundwater head with observed heads. Results of integrated surface-groundwater model also help better decision making. WISDOM uses the very popular – modular hydrologic simulation program called MODFLOW – developed by U.S Geological Survey. MODFLOW discretizes the area of interest into several grids, control-volume units, to generate finite-difference equations. The finite-difference equations are formulated for intercell flow, boundary conditions and specified flows in terms of conductance. MODFLOW simulates groundwater flow in 3-dimensions using the Darcy's Law as described below.

$$q = -K\nabla h = \begin{pmatrix} K_{xx} & 0 & 0 \\ 0 & K_{yy} & 0 \\ 0 & 0 & K_{yy} \end{pmatrix} \tag{2.27}$$

Where q is specific discharge, K is hydraulic conductivity, sub-scripts xx, yy and zz indicates hydraulic conductivity in x, y and z directions, h is groundwater potential head. When combined with a water balance on a small control volume, Darcy's Law leads to a partial-differential equation that describes the distribution of hydraulic head:

$$\frac{\partial}{\partial x}\left(K_{xx}\frac{\partial h}{\partial x}\right) + \frac{\partial}{\partial y}\left(K_{yy}\frac{\partial h}{\partial y}\right) + \frac{\partial}{\partial z}\left(K_{zz}\frac{\partial h}{\partial z}\right) + Q_s = S_s\frac{\partial h}{\partial t} \tag{2.28}$$

where Q_s is a volumetric flux per unit volume representing sources and sinks of water, with Qs being negative for flow out of the groundwater system, and Q_s being positive for flow into the system. S_s is the specific storage of the porous material and t is time.

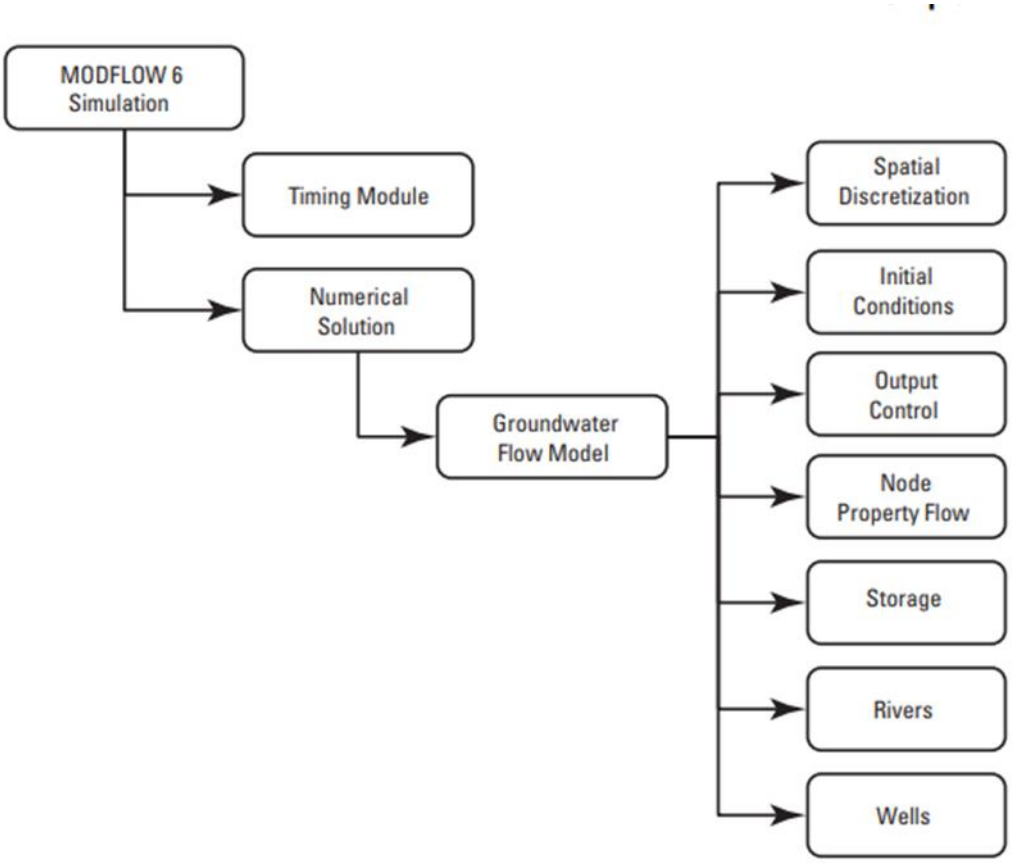

Figure 2.4. MODFLOW components for groundwater flow simulation

Under real world conditions, the analytical solution of Partial Differential Equations (PDEs) of groundwater flow is rarely possible, therefore the CVFD (Control Volume Finite Difference) method is used in MODFLOW. In CVFD, the continuous system described by PDEs is replaced by a finite set of discrete points in space and time, and the partial derivatives are replaced by terms calculated from the differences in head values at these points. The process leads to a system of simultaneous linear algebraic difference equations; the solution yields values of head at specific points and times. These values constitute an approximation to the time-varying head distribution that would be given by an analytical solution of the partial-differential equation of flow. The CVFD analog of PDEs may be derived by applying the rules of difference calculus; however, in the discussion presented here, an alternative approach is used with the aim of simplifying the mathematical treatment and explaining the computational procedure in terms of familiar physical concepts regarding the flow system. In MODFLOW 6, the discrete control volumes that comprise the model domain are called model "cells." Within each cell there is a point called a "node" at which head is to be calculated. Many schemes for locating nodes in cells could be used; however, the finite-difference equation developed in MODFLOW uses the block-centered formulation in which the nodes are at the center of the cells. Hydraulic communication between cells is conceptualized in terms of conductive

connections between nodes. The assemblage of model cells and its associated network of connections is called the model "grid." To get further description of theory of MODFLW, readers are recommended to refer to the MODFLOW documentations (Langevin, et. al., 2017)

In WISDOM, the MODFLOW integration mainly aims at the groundwater flow simulation in multi-layer groundwater system. To achieve this object, the required MODFLOW packages are selected and integrated in WISDOM (Table-2.1). Each MODFLOW module needs input files in specified format which consists of various options to activate/deactivate MODFLOW functions, package specific parameters, stress period data and time-series data. These inputs files can be created manually for real-case problems, and therefore, an automated process is required. WISDOM derives file for all the modules utilizing various distributed inputs, daily time-series, and user specified options and parameters. It also allows transformation of data from user uploaded excels and shape files. The input preparation for MODFLOW is WISDOM utilizes various python programs and a python library, called FloPy.

The MODFLOW discretizes the model domain into grids to consider spatial variations in various aquifer characteristics and to obtain solution of partial differential equations. The 3D schematic of MODFLOW is shown in Figure 2.5 which illustrates the computation nodes, aquifer layers and active/in-active cells. MODFLOW writes output in binary and text files which can't be analysed directly. WISDOM reads all MODFLOW output files and convert to excel so that the time series and thematic outputs can be visualized latter in WISDOM's dashboard.

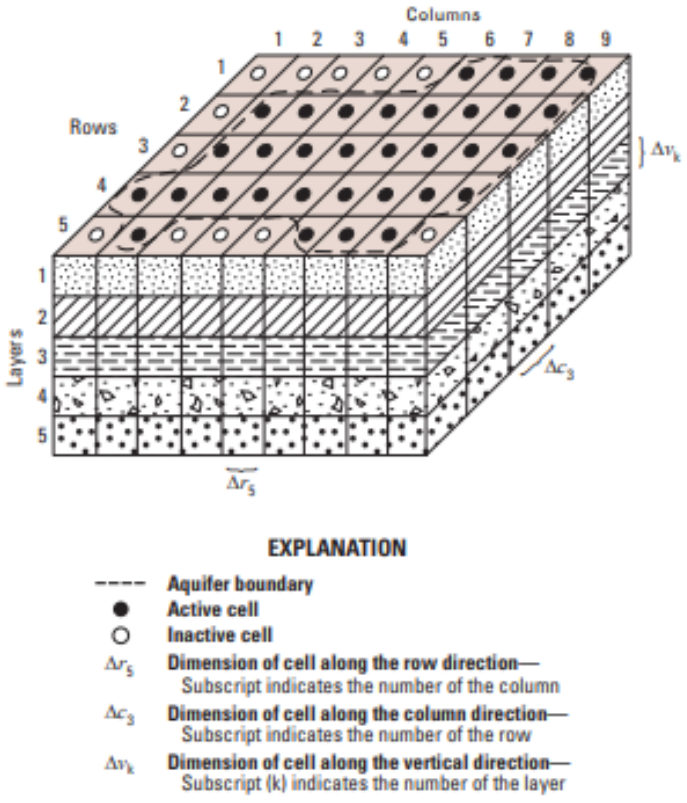

Figure 2.5. Spatial discretization in MODFLOW (Source: Langevin, et. al., 2017)

Table – 2.1. MODFLOW modules used in WISDOM

Sr. No.	MODFLOW Module	Description
1	DIS6	Discretization package
2	NPF6	Node Property Flow Package Pane
3	STO6	Storage Package
4	UZF	Unsaturated-Zone Flow package
5	SFR6	Stream-Flow Routing package
6	WEL6	Well package
7	GHB6	General Head Boundary package
8	CHD6	Time-Variant Specified Head package

2.4 PEST

Integrated models use several hydrologic equations which have parameters that cannot be determined directly in the field through in-situ measurements. Such parameters are generally calibrated by comparing the simulated and observed hydrologic components, such as river discharge and groundwater head. However, for integrated hydrologic models, the parameter estimation becomes very complex as these involves a large number of parameters (say, 10 to 100) and manual tuning of such large set of parameters seems impossible. Therefore, it is wise to integrated optimization algorithms with such complex models to automate calibration procedure. PEST - Model-Independent Parameter Estimation and Uncertainty Analysis – is an open-source FORTRAN program that support auto-calibration of complex hydrologic models. It also allows parameter sensitivity and uncertainty analysis. PEST is integrated with the integrated model in python environment. The interface of PEST will be provided in the next version of WISDOM.

2.5 System Components

The WISDOM may be divided into five broad components, namely GEE-based cloud computing, model data preparation, simulation, visualization and dissemination (Figure 2.6). All these components are closely integrated to simulated various surface and subsurface processes.

2.5.1 GEE-based cloud computing

Google Earth Engine (GEE) is a free cloud-based platform that makes it easy to access high-performance computing resources for processing very large geospatial datasets. Moreover, it allows to access and analyze various remote sensing data available from various organizations throughout the world. A number of GEE data products are used in the model, such as precipitation, LAI, impervious surface, land cover, soil, etc. All these data sets are processed first on the GEE server and rescaled at model grid for the period and area of interest.

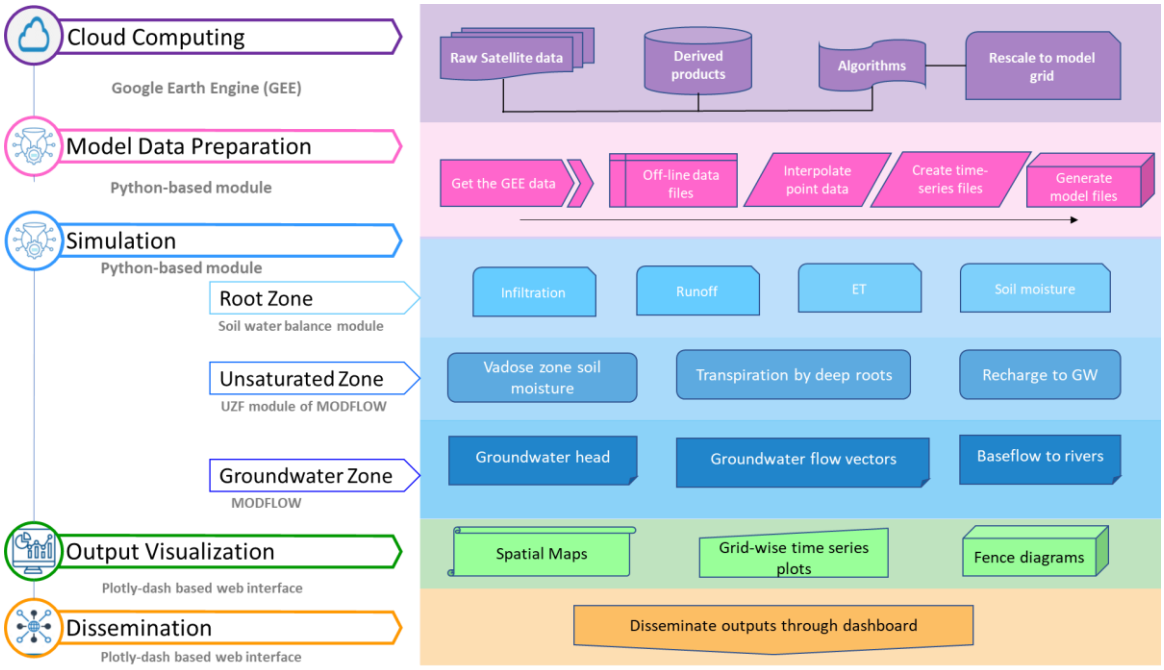

Figure 2.6. System components and sub-components

2.5.2 Model data preparation

The data preparation module is developed to convert GEE data to model format. Since there are some data which are to be given off-line, such as aquifer geometry, parameters, observed groundwater heads, etc. These data sets are interpolated to create required surface layers. All such data files are then converted to model files.

2.5.3 Simulation

This mainly includes the integrated surface-subsurface model which consists of RZF, UZF and GWF modules. These models are integrated in such a way that the input-output are shared amongst them for integrated simulation. All these models are mainly governed by a control script written in Python. Several libraries were also used in this module, such as fllopy, gdals, pandas, geopandas, numpy, etc.

2.5.4 Output Visualization

This module is mainly created to visualize the inputs and outputs of the model. It includes interactive maps and plots. All the thematic and time-series outputs can be visualized. It also allows on-click plotting so that any variable can be plotted for any grid when click over the map. The maps and plots can also be downloaded in *jpg* format.

2.5.5 Dissemination

After each successful run of model, the WISDOM creates dashboard-like interface for output visualization. This dashboard can be made public on the web with few customizations in the python script.

2.6 Web-based Interface

A few snapshots of the developed interface are shown in the Figures 2.7 to 2.13

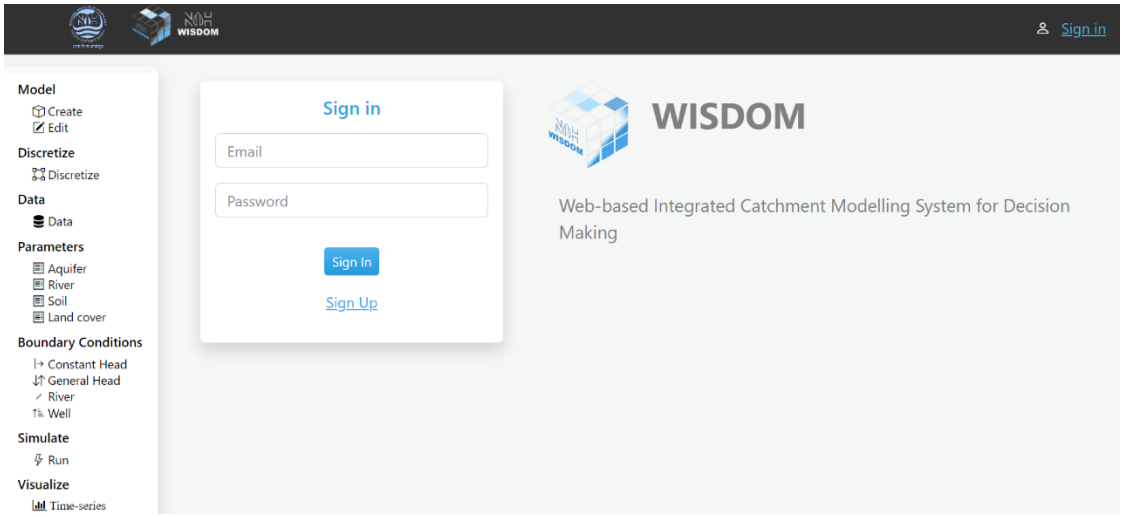

Figure 2.7. Login page: Options to register or Sign-in is given. After log-in, users are re-directed to *Edit* page where all the models developed by the user are displayed. User is allowed to delete or edit any of the listed models.

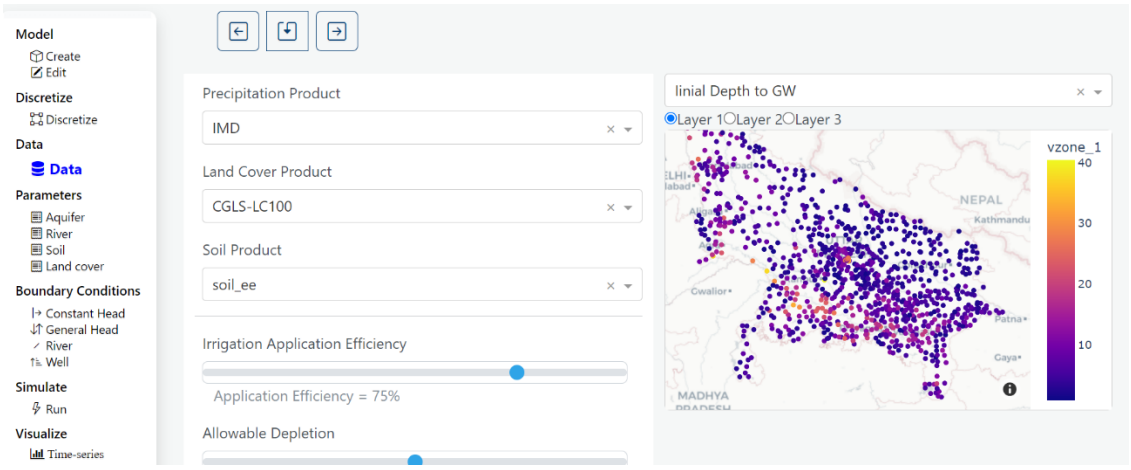

Figure 2.8. Data upload page. In the left, various options to select data products for precipitation, land cover and soil are provided. Options to change *irrigation application efficiency* and *allowable depletion* can also be assigned. In the right, a map is provided to visualize various groundwater data uploaded by user.

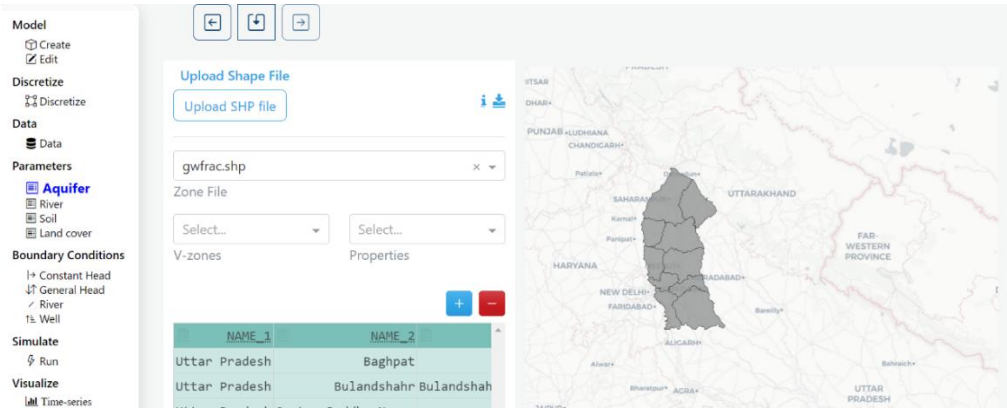

Figure 2.9. Aquifer: zone-wise aquifer details can be uploaded here. A shapefile with required attributes is uploaded. User can add / delete attributes to assign zone-wise aquifer parameters

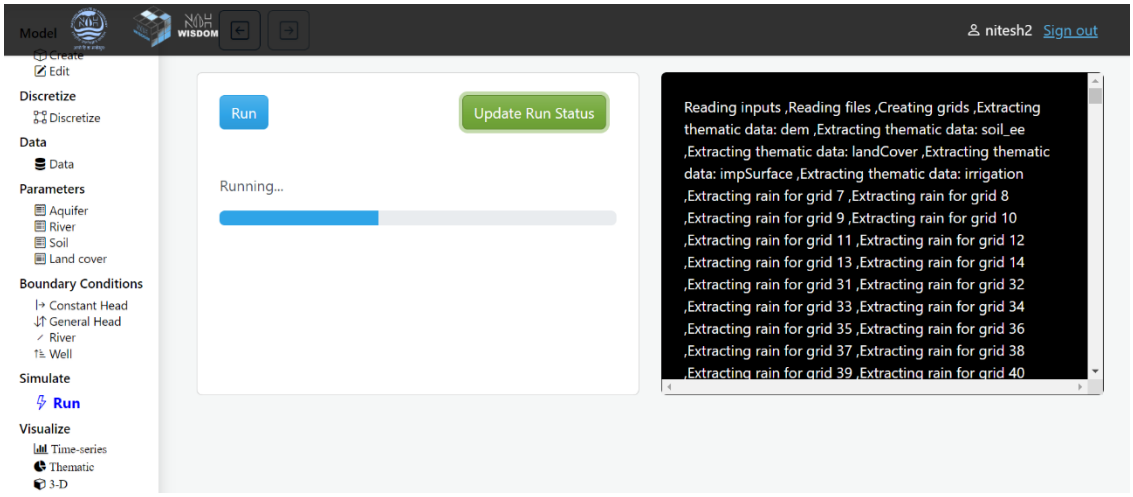

Figure 2.10. Model run: The model can be run after all inputs are prepared. The run button ques the model for simulation. The run status can be updated by pressing the *Update Run Status* button.

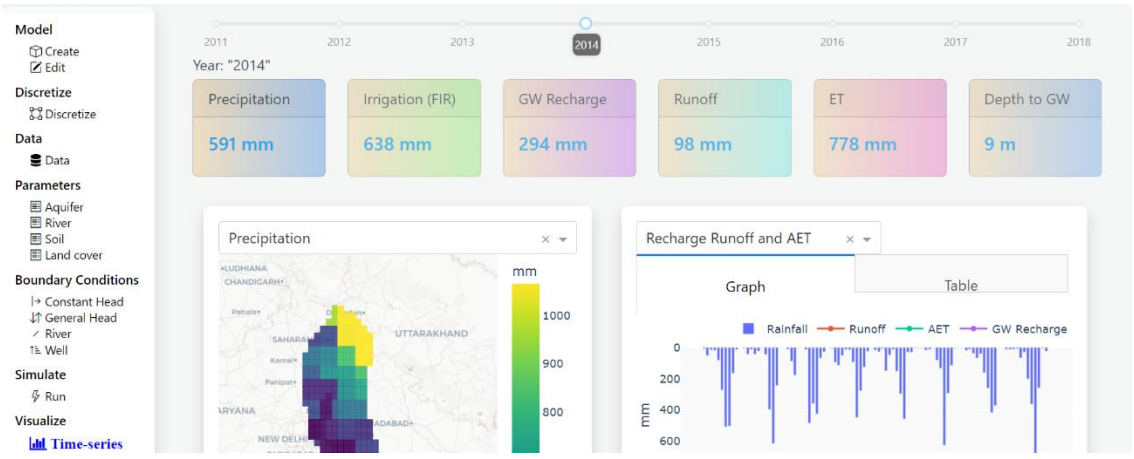

Figure 2.11. Time-series outputs: The inputs and outputs can be visualized here in the form of spatial maps and time-series plots. The annual maps of all the time series variables are generated. A monthly time-series can be plotted for any grid by clicking on the map.

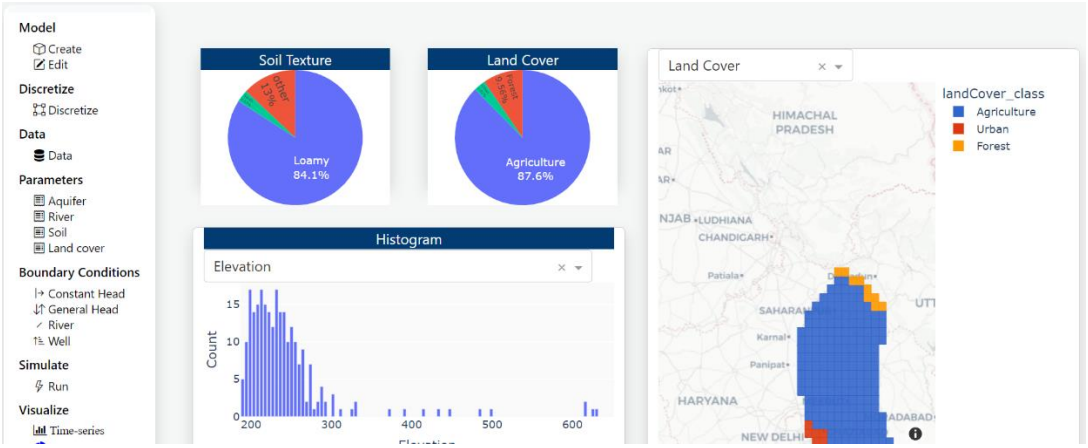

Figure 2.12. Thematic outputs: The thematic layers, such as land cover, soil, elevation, etc., can be visualized here in the form of maps, histogram and pie charts

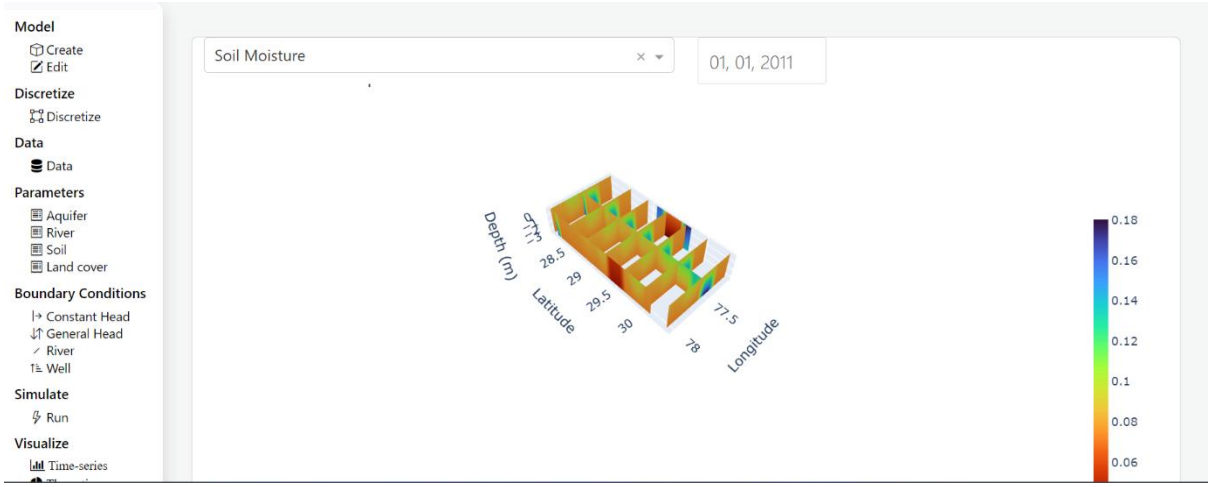

Figure 2.13. 3D outputs: 3D Fence diagrams for aquifer layers and soil moisture can be generated. Date can be changed for Soil moisture diagram.

***

Chapter-3
STUDY AREA

The NIH-WISDOM is applied in Hindon river basin and upper Mahanadi River basin to verify the simulated surface-subsurface hydrological fluxes. A more comprehensive model testing was performed in the Hindon basin to simulate groundwater recharge, groundwater head, soil moisture, etc. To assign the boundary conditions appropriately, the model domain for Hindon is extended to river Yamuna in the West and river Ganga in the East. The extended domain is referred hereafter as upper Ganga Yamuna Doab. While, to test the runoff simulation capability, application in upper Mahanadi basin is performed as consistent discharge data was not available in Hindon river basin. Detailed description of these basins is provided in the following sections.

3.1 Hindon River Basin

River Hindon originates from Saharanpur district of Uttar Pradesh and joins river Yamuna near Delhi. The basin lies between the latitudes 28°30′15″ to 30°15′12″ N and longitudes 77°20′18″ to 77°50′10″ E and has an area of ~7000 km^2 (Figure 3.1). It is largely composed of Pleistocene and Quaternary alluvium represented by sand, clay and kankar. Hindon basin lies in the Ganga-Yamuna doab region – the interfluvial region between river Ganga and Yamuna – where river Yamuna flows in the West and Ganga in the East. The main channel of river Hindon is approximately 206 km long traverse through five districts of Uttar Pradesh, namely Muzaffarnagar, Meerut, Baghpat, Ghaziabad and Gautam Budh Nagar. It joins river Yamuna in Noida, NCR. River Kali and Krishnai are the two major tributaries of river Hindon. Kali originates from Rajaji Range of Shivalik Hills and is known to be highly polluted as it traverses through the industrial belt of Uttar Pradesh. Since past few years, groundwater abstractions to meet the agricultural needs have led to depleted groundwater levels in the area. These depletions have not only reduced the groundwater availability but also have made the groundwater more susceptible to pollution and have reduced the baseflow contribution to the streams. The alarming groundwater declines, emerging groundwater quality issues and ever-increasing water demand in the region necessitate proper planning and management of groundwater resources. This requires precise quantification of groundwater recharge, assessment of various recharge/abstraction scenarios on groundwater system and implementation of water management strategies. As the groundwater is a dynamic resource which varies with the recharge and extraction, frequent assessments are needed for better planning.

3.2 Land use and land cover

Hindon is an agriculture dominated basin with agriculture area of around 90%. The forest and urban each occupy around 5% area of the basin. Rice, sugarcane and wheat are the main crops in the basin. The area is also known for orchard cultivation, mainly including Mango orchards, although the total orchard/plantation area is less than 1% of the basin. The Northern portion of the basin lies in the Himalayan outer foothills – the terai region – which is occupied by the tropical moist deciduous forest. The part of National Capital Region (NCR), most of which is

dense urban settlement, is also lies in the Southern portion of the basin. An industrial belt in the Saharanpur district is also the part of Hindon basin.

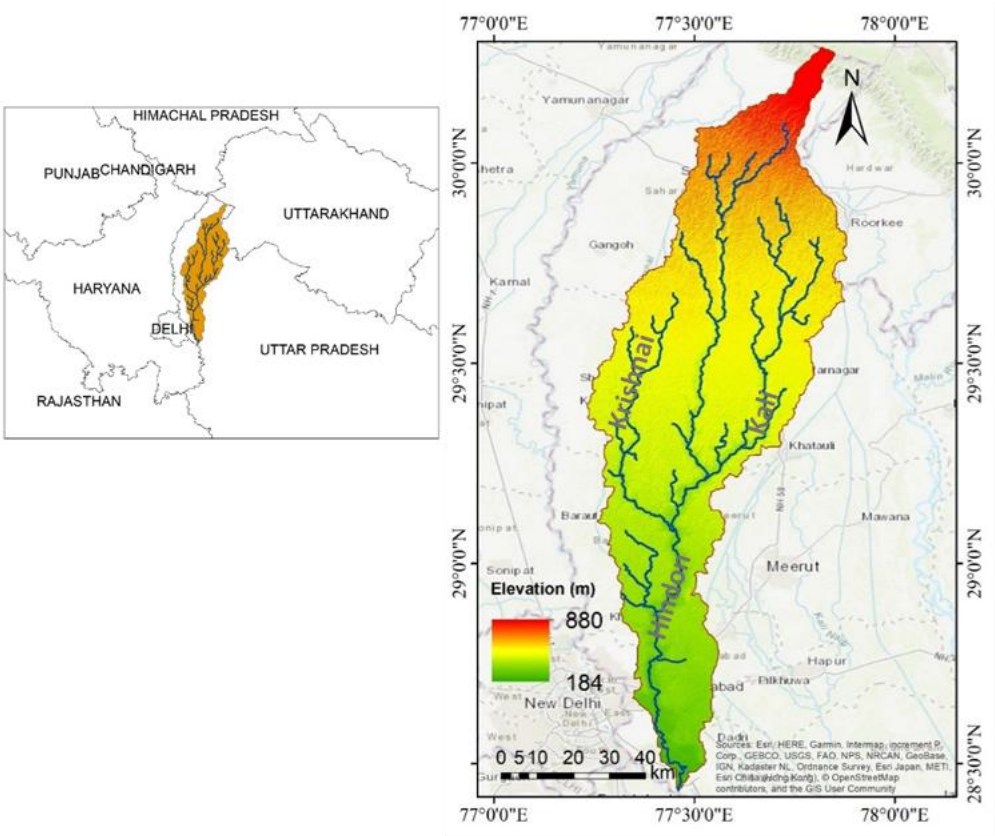

Figure 3.1. Hindon river basin with elevation and stream network

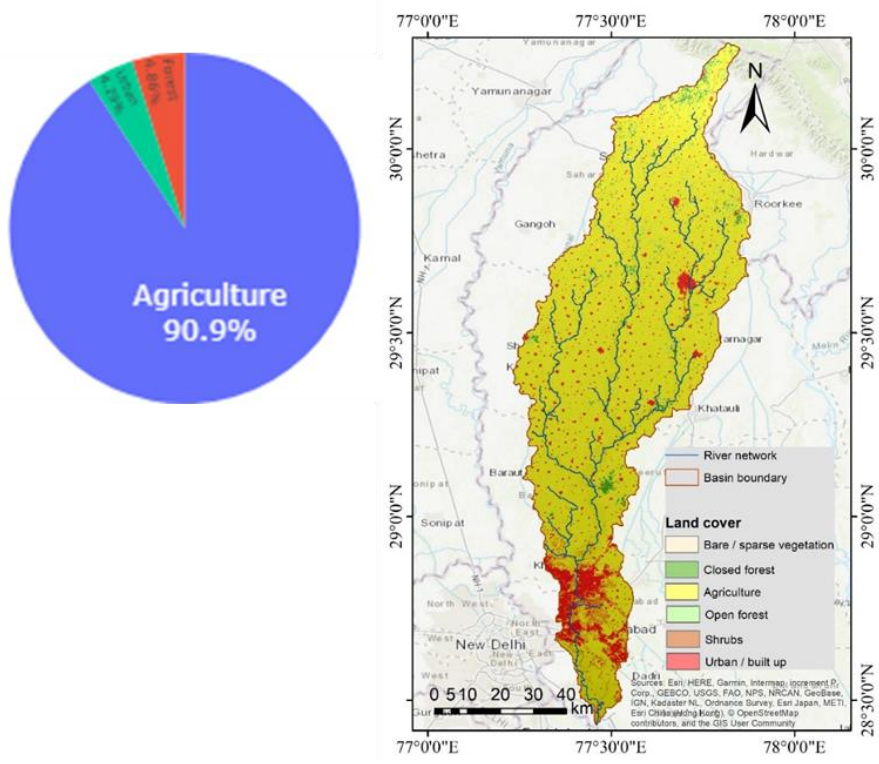

Figure 3.2 Land use and land cover map prepared using Copernicus 100 m data

3.3 Soil

Most of the basin area is covered by *Coarse Loamy* soil with few patches of *Fine Loamy*. Few small patches of *Sand* are also seen in the basin. The soil texture map of the study area as prepared using the soil map of National Bureau of Soil Survey and Land Use Planning (NBSS & LUP) is shown in Figure 3.3.

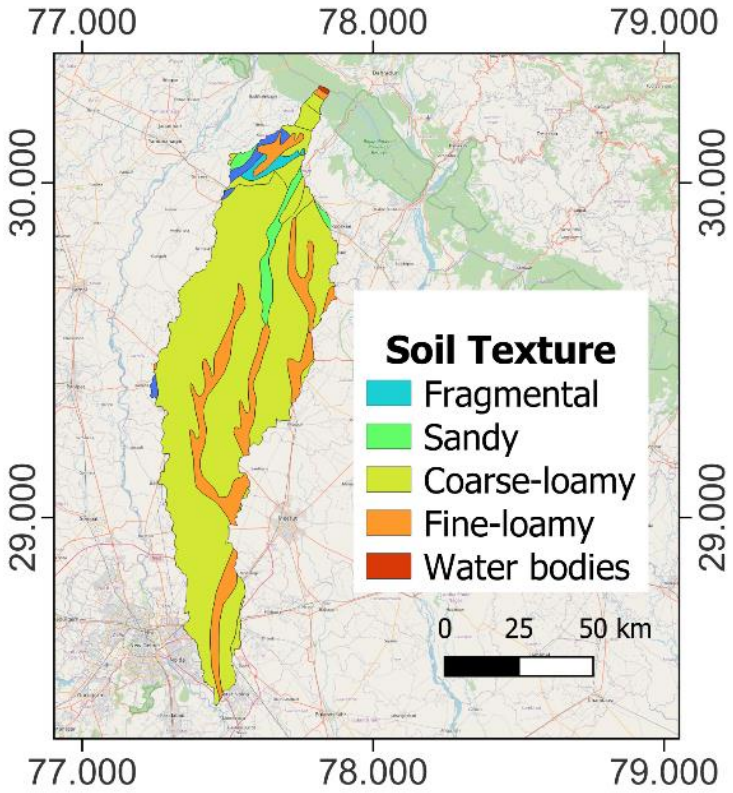

Figure 3.3 Soil texture map of Hindon river Basin

3.4 Hydro-geological Set-up

The study area is in the Gangetic basin built-up of the gravel, sand and clays of quaternary age in alternation. The flexing lithosphere controlling thickness of the alluvial fill and affecting river channel on surface shows many inhomogeneities below Ganga plain in the form of ridges (e.g. Delhi-Haridwar ridge) and basement faults.

The available sub-surface data up to a depth of 122 m indicates a persistent top clay layer of depth 3 to 20 m throughout the area underlained by a more porous granular zone(Umar et al., 2009). The study area is underlain by Quaternary alluvium of 2 cycles of sedimentation- the older one is of Late - Middle Pleistocene covering most of study area and the younger one is of Late Pleistocene - Holocene where in the vicinity of river channels newer alluvium has been confined. The area has 3 distinct groups of aquifers up to 463 m BGL with top sandy clay bed with thickness of 5 to 35 m; 1st aquifer continues down to 162 m BGL; 2nd aquifer occurring between 145 m BGL - 327 m BGL; 3rd aquifer lies between 288 - 463 m BGL (CGWB, 2017).

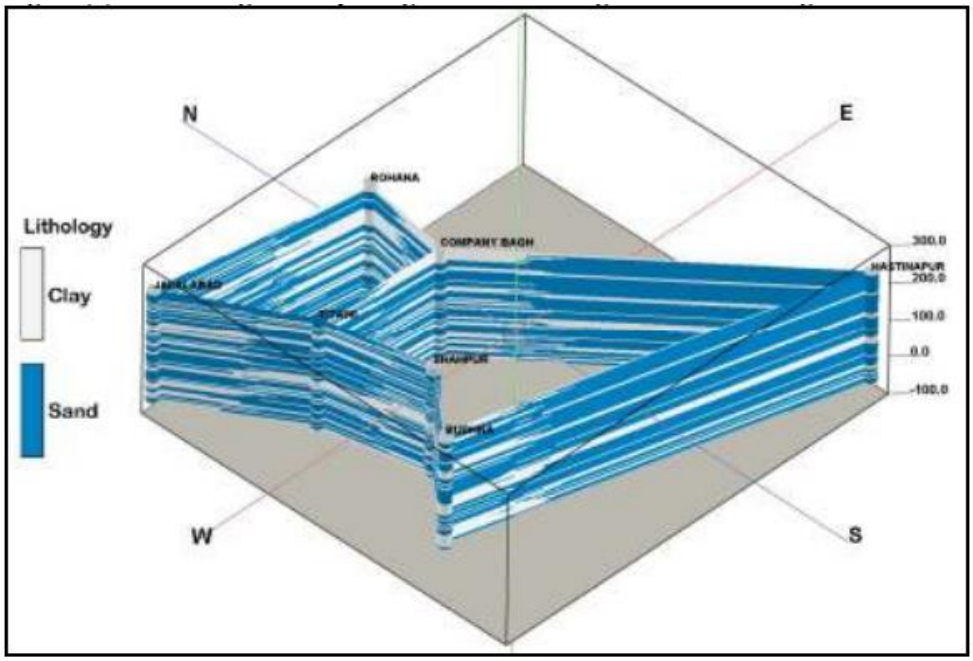

Figure 3.4 Sub-surface lithological variations (Source: CGWB)

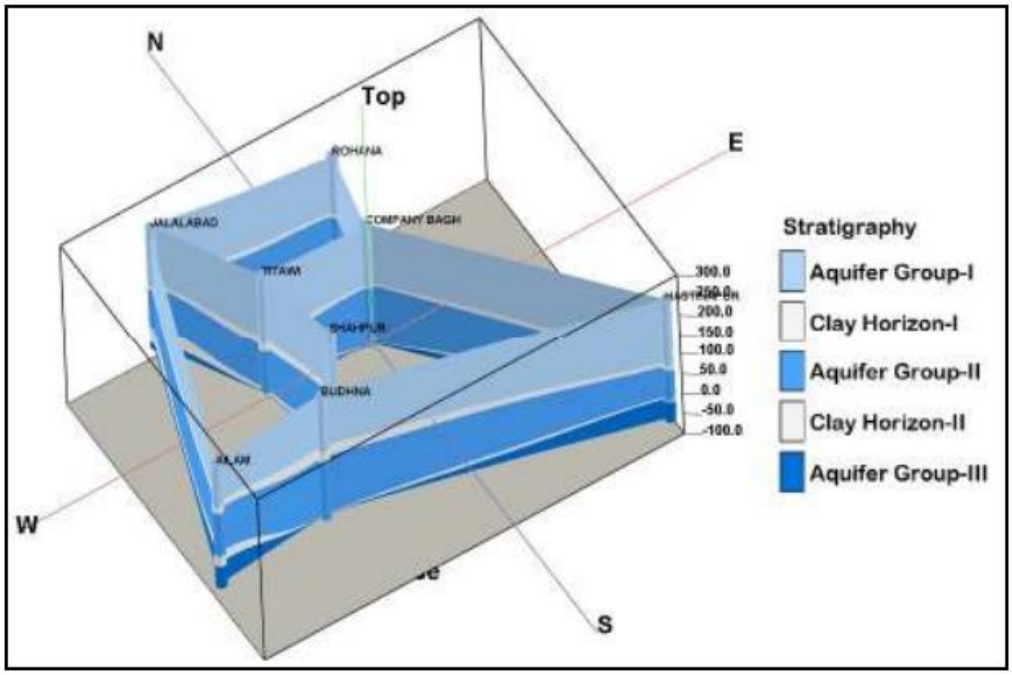

Figure 3.5. Fence diagram depicting sub-surface regionalized aquifers (Source: CGWB)

There is occurrence of phreatic shallow aquifers and semi-confined to confined deeper aquifers with rainfall as the main ground water recharge source. The groundwater also gets recharge from irrigation-return flow and seepage from the canal networks. The aquifers with transmissivity of 1265–4003 m^2 /day and hydraulic conductivity of 9.8–26.6 m/day are evolved in fluvial system. The channel deposits of aquifers form most potential groundwater reservoir, while the flood plain deposits are only with moderately potential.

3.5 Climate

The annual precipitation varies in the basin from ~600 mm (near Delhi) to ~1300 mm (in the Teria region). Precipitation map of the year 2011 is shown in Figure 3.6 with monthly precipitation in the Northern, Central and Southern parts of the basin. The monthly pattern of precipitation is similar throughout the basin, although the magnitude varies considerably from North to South. It can be seen from the monthly bar plots that more than 80% of annual precipitation occurs during the monsoon season, mainly during July, August and September. The temperature also varies considerably in the basin. The Northern portion of the basin generally colder than the Southern parts. The year highest temperature is observed during summer season (mainly during April, May and June). Near Delhi NCR, the year-highest temperature is 42°C with minimum temperature of 32°C, while in the northern portions, it is observed in the range 25°C (min) to 35°C (max).

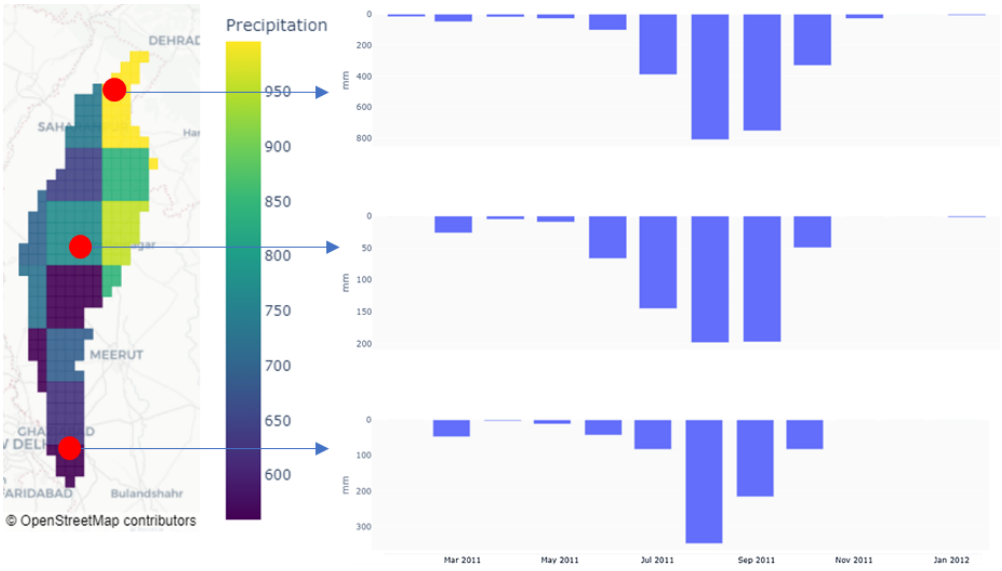

Figure 3.6. Precipitation in Hindon river basin during 2011.

3.6 Status of Groundwater

Groundwater level varies considerably in the study area. In the Northern portion, depth to groundwater varies in the range 2 to 8 m BGL (Below Ground Level). The middle portions have relatively deeper depth to groundwater as compared to both the Northern and Southern portions. Central Ground Water Board (CGWB), Govt. of India, monitors groundwater quarterly during Monsoon (Jul-Sep), post-monsoon Kharif (Oct-Dec), Post-monsoon Rabi (Jan-Mar) and pre-monsoon (Apr-Jun). Seasonal groundwater fluctuations at various locations in the study area are shown in Figure 3.7. Evidently, the groundwater has declined at an alarming rate in the Central parts of the study area. While, in the Northern and Southern parts, the rate of decline is relatively low. Seasonal variations in the entire study area are considerable. During the monsoon, groundwater rises due to recharge from precipitation and starts declining during post-monsoon due to groundwater pumping for irrigation, leading to the deepest groundwater during pre-monsoon season. Consistent decline in groundwater in the central parts of the study area is alarming and needs urgent measures to constrain and restore the depletion so that long-term groundwater availability could be ensured in the region.

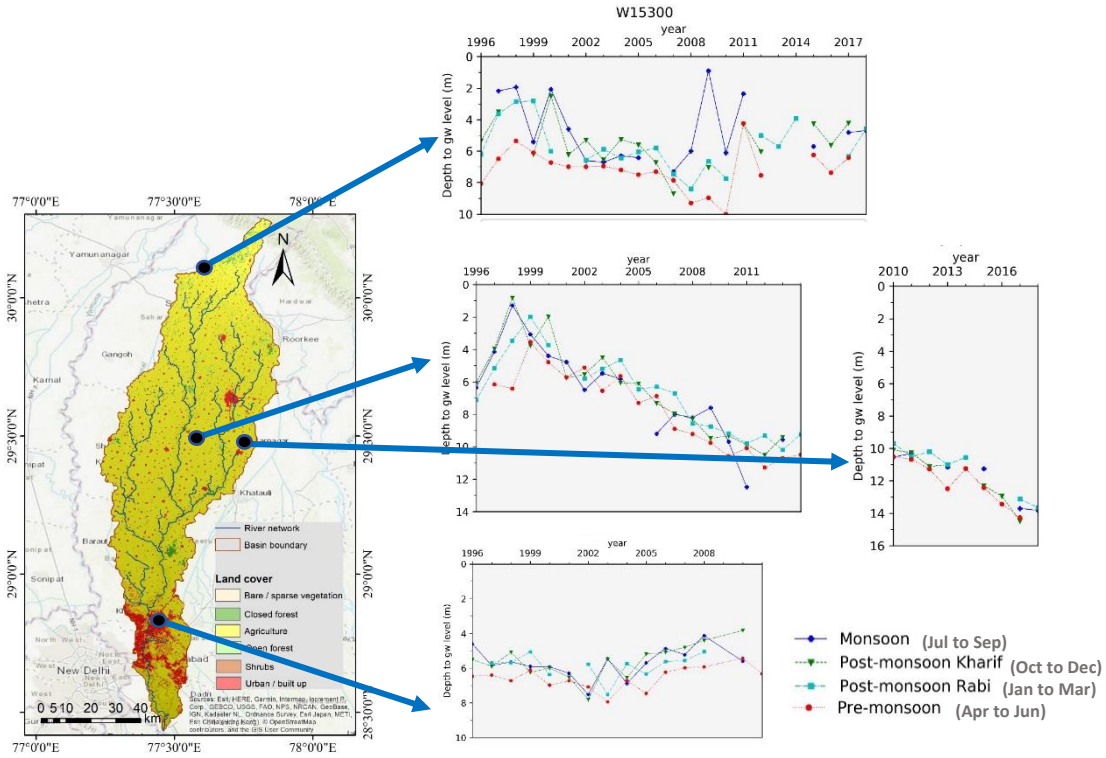

Figure 3.7. Depth to groundwater at various locations in the study area

3.7 Trend in groundwater levels

Trend analysis was performed on the selected 28 wells, on annual scale using modified Mann-Kendall (M-K) test (Hamed & Rao, 1998). The Mann-Kendall test is a non-parametric test for identifying trends in time series data. Being non-parametric, it allows to perform trend analysis on any distribution of data. Values are evaluated as an ordered time-series. Each value is compared to all subsequent values. The initial value of the Mann-Kendall statistic, S, is assumed to be 0 (e.g., no trend). If a value from a later time period is higher than a value from an earlier time period, S is incremented by 1. On the other hand, if the data value from a later time period is lower than a value sampled earlier, S is decremented by 1. The net result of all such increments and decrements yields the final value of S. Further, in order to test the significance level, a probability test is integrated with the M-K test. In this study, the modified Mann-Kendall (M-K) test developed by Hamed and Rao (1998) was used. An annual time series from 2011 to 2020 of depth to GW was created and used in the modified M-K test. Wells with rising and falling GW level were identified at a significance level of 0.05.

On annual scale, the majority of wells (60%) show no-trend, while 40% of wells have falling trend (Figure 3.8). The wells with no-trend are mainly in the Northern parts while the wells with falling trends are in the middle and Southern portions.

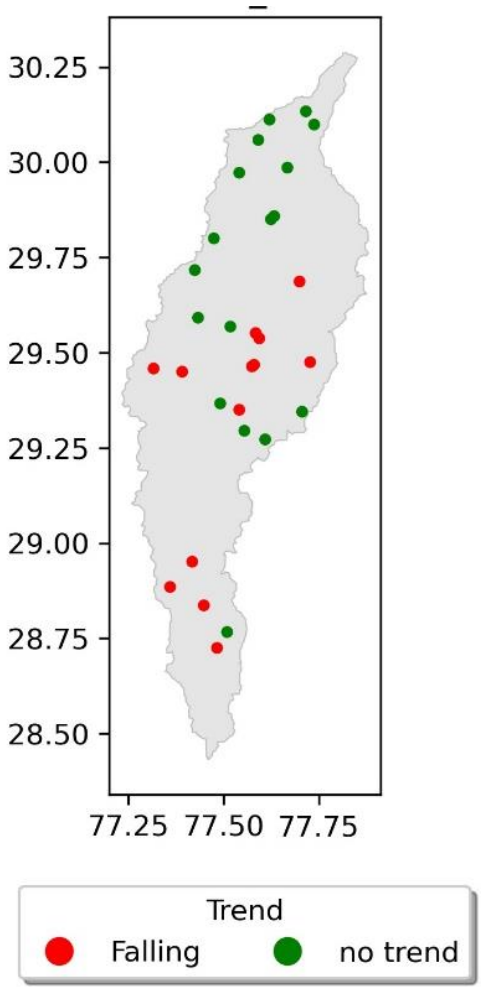

Figure 3.8. Trend in depth to GW during 2011-20

3.7.1 Seasonal variations

Spatial map created by interpolating the well observations of recent decade (2011-2020) for Pre-monsoon season shows that Northern parts have depth to GW in the range of 7 to 12 m. Middle portion have slightly deeper GW which ranges from 12 to 14 m. White the Southern and Western parts have deeper GW with depth from 14 to 20 m (Figure 3.9). During monsoon season, the GW table shows considerable rise due to recharge from rainfall. The Northen parts show depth to GW in the range of 6 to 9 m. Middle portion have the depth to GW from 8 to 12 m. The Southern and Western parts show depth to GW in the range of 14 to 17 m. During post-monsoon Kharif (POMKH) season, the water table starts falling due to GW pumping. The spatial pattern is similar to the monsoon season with slightly deeper depth to GW. During the post-monsoon Rabi (POMRB), the depth to GW declines further due to GW pumping.

3.7.2 Annual average

Annual GW levels (average of all seasons) have also been analyzed. Spatial pattern at annual scale looks similar to other seasons. Depth to GW varies in the range of 7 to 10 m in the Centre while in the Western and Southern parts it ranges from 14 to 18 m.

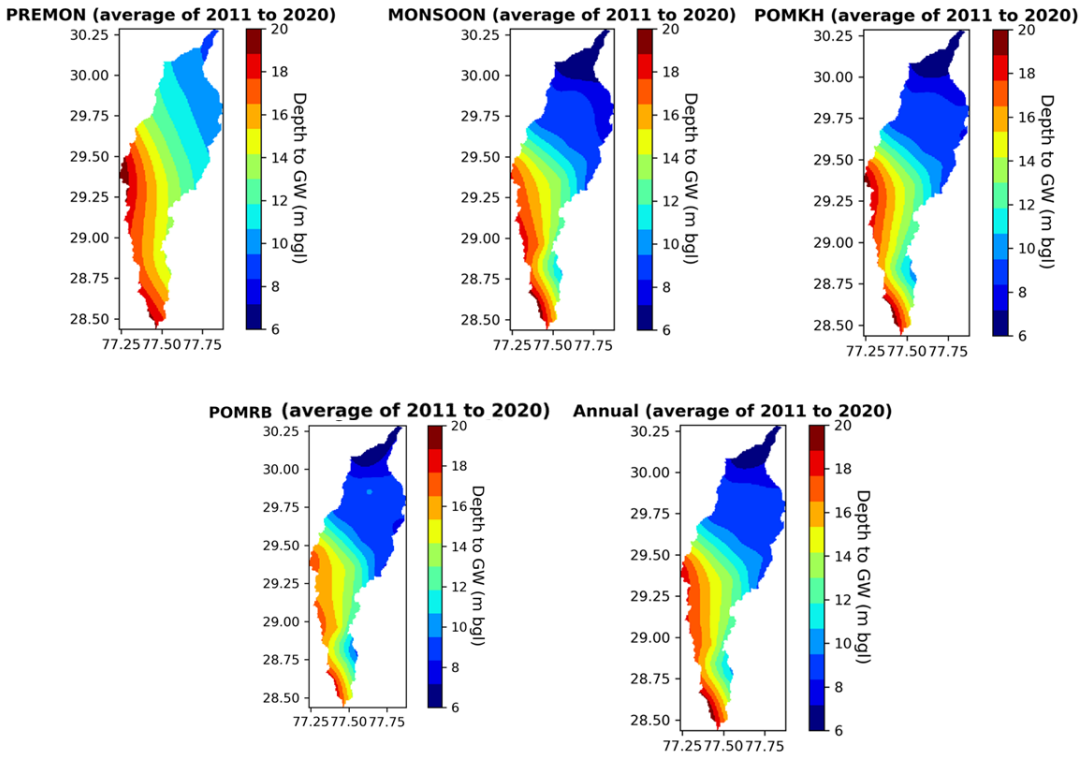

Figure 3.9. Depth to GW in different seasons (average of previous decade)

3.8 Ganga-Yamuna Doab

The Ganga-Yamuna doab is a part of Indo-Gangetic plain covering the area between rivers Ganga and Yamuna. It extends from Teria region in the North to Delhi in the South. The total geographical area of the study area is around 20,386 km^2. The river Hindon traverse through the middle of the study area which joins river Yamuna near Delhi. The area is one of the densely populated regions of India and falls in the states of Uttar Pradesh, Haryana, Uttarakhand and Delhi. It is mostly consisting of flat terrain with agricultural fields. A small part of the study area consists of hilly terrain which is occupied by forest. Paddy, Sugarcane and Wheat are the main crops of the area. The National Capital Region (NCR) Delhi, which is one of the densely populated cities and a commercial hub of India, partially lies in the study area. The increased groundwater utilization for irrigation, domestic and industrial purposes during the past decades has led to declined groundwater levels in the area. Further, it is envisaged that the water demand would further be amplified in future to cater population growth and agriculture expansions which may further increase the pressure on groundwater of the area. In order to maintain a balance between the groundwater extraction and replenishment, Managed Aquifer Recharge (MAR) may be considered as an ameliorative measure in the area.

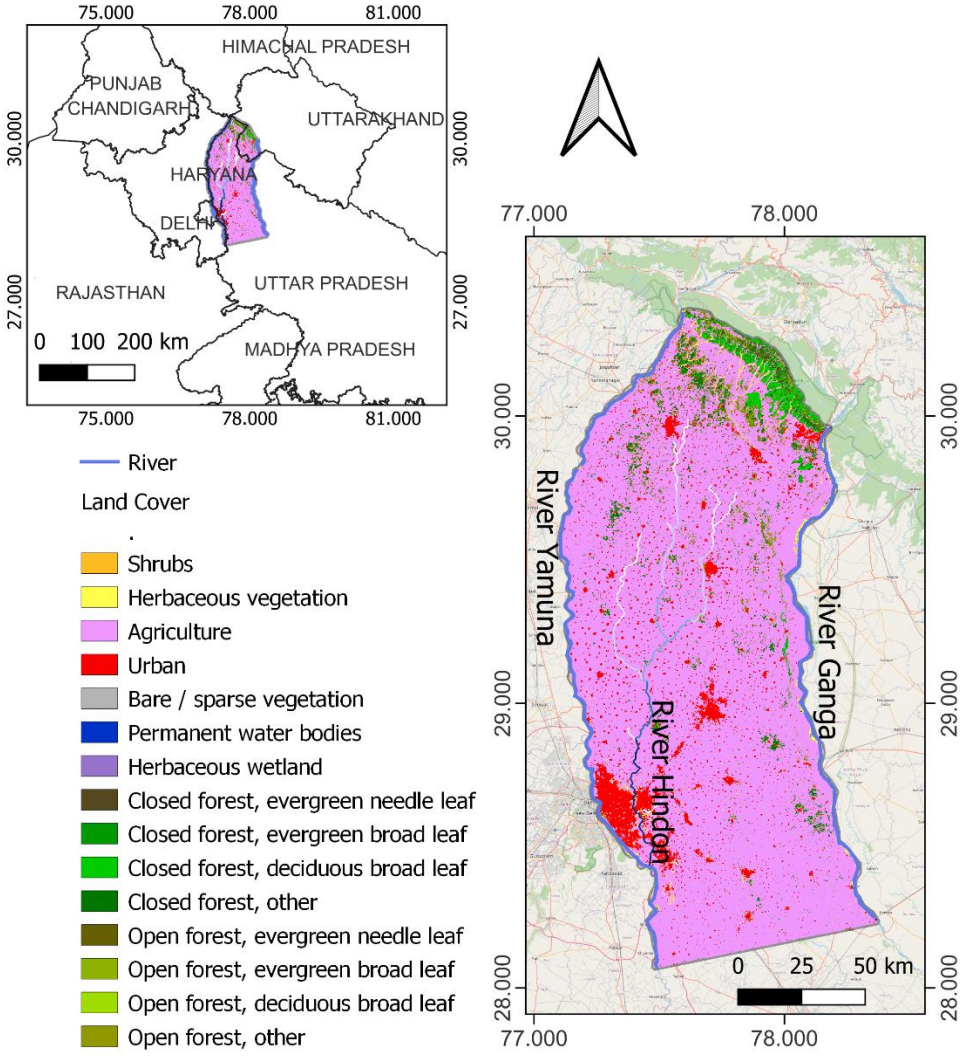

Figure 3.10 Study area: Location and land cover

3.9 Upper Mahanadi Basin (up to Basantpur)

The Upper Mahanadi Basin is selected as a test basin for streamflow simulation. Upper sub-basin of Mahandi basin was delineated by selecting Basantpur as the outlet. Basantpur is located in the river Mahanadi in the upstream of Hirakund dam (Figure 3.11). The approximate distance of Basantpur from the Hirakund is 80 km. The test basin has an area of 58,012 km^2. The area is dominated by agricultural lands with considerable coverage by deciduous forest.

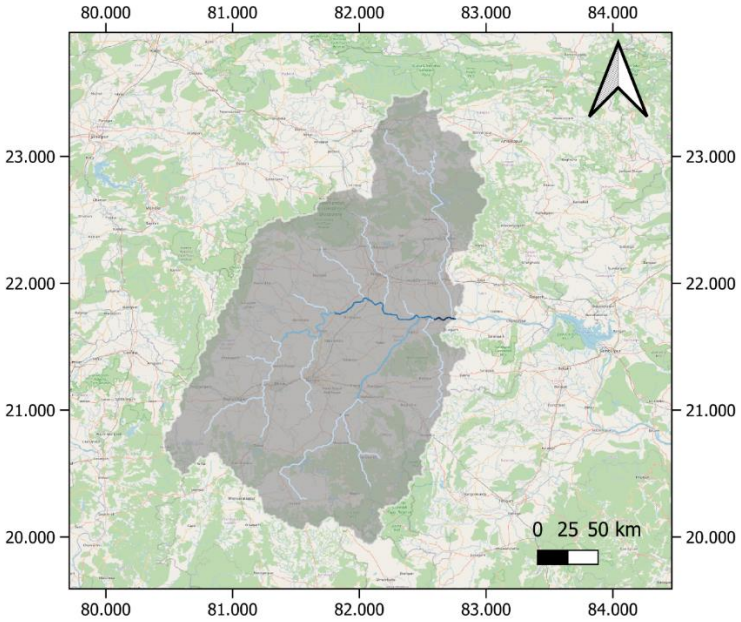

Figure 3.11 Upper Mahanadi basin up to Basantpur

3.9.1 Topography, soil and land cover

Elevation in the upper Mahanadi basin varies from 269 to 527 m above mean sea level (Figure 3.12). The basin is bounded by hills in North and South. The area is mainly dominated by agricultural lands which is situated in the central portion (Figure 3.13). The Hilly regions in the North and South are occupied by forest. Few small patches of urban and waterbodies are also presents. The basin is having mainly Loamy and Clayey soil textures with small patches of Loamy skeletal (Figure 3.14).

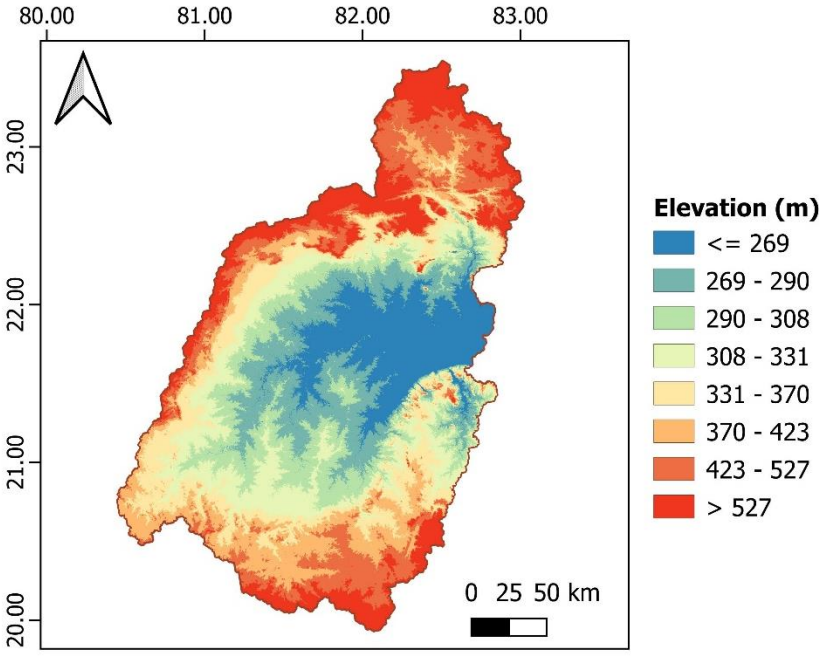

Figure 3.12. Elevation (m AMSL) in the upper Mahanadi Basin

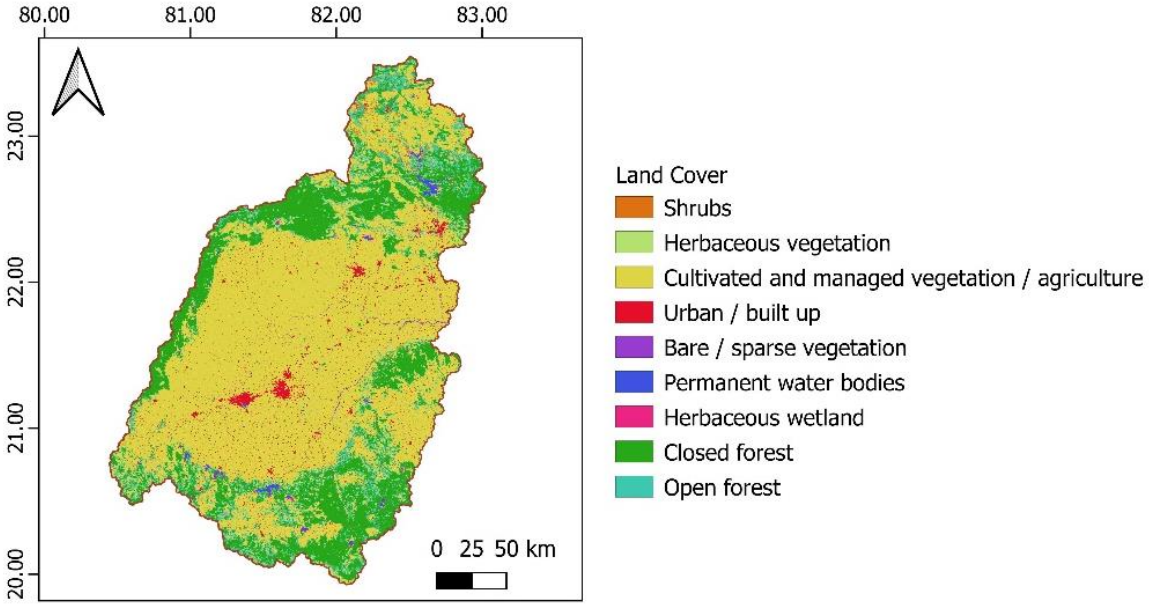

Figure 3.13. Land cover in the upper Mahanadi Basin

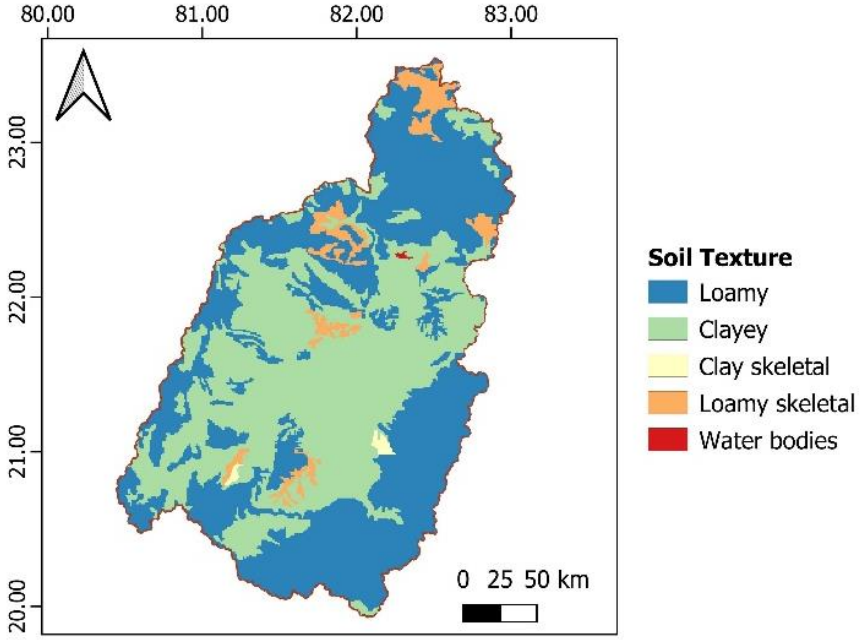

Figure 3.14. Soil texture in the upper Mahanadi Basin

***

Chapter-4

MODEL APPLICATION

The WISDOM is applied in Ganga-Yamuna doab (GYD) and Upper Mahanadi Basin (UMB) for simulating surface-subsurface hydrologic components. The application in GYD was focused on the simulation of groundwater recharge and groundwater head, while the more detailed testing for runoff simulation was conducted in UMB.

4.1 Model setup in GYD

The WISDOM was setup at 5 km grid resolution and daily time-step for integrated surface-groundwater modelling. The grid-based input files for RZF and MODFLOW were generated in WISDOM using various GEE data, IMD data and uploaded aquifer data. Details of the inputs used are provided in the following sub-sections.

4.1.1 Thematic layers

The thematic layers, including land cover, soil texture, elevation, aquifer depths and aquifer parameters are created using either the GEE data or by interpolating uploaded point data. The GEE/interpolated layers were then aggregated to model grids.

Table-4.1. Thematic and time-series data products used in modelling

Sr. No.	Data	Description	Source
		Thematic data	
1	Land Cover	Land cover map of 100 m resolution (CGLS-LC100)	GEE
2	Soil	Soil texture map of National Bureau of Soil Survey and Land Use Planning (NBSS and LUP)	NBSS&LUP
3	Elevation	Shuttle Radar Topographic Mission (SRTM) 90 m	GEE
4	Aquifer type and depth	Derived from National Aquifer Mapping Mission (NAQUIM) reports	CGWB
5	Irrigated area	Global Food Security-support Analysis Data at 30m Project (GFSAD30)	GEE
6	Impervious surface fraction	GHSL: Global Human Settlement Layers	GEE
		Time-series data	
7	Precipitation	Gridded 0.25-degree data of India Meteorological Department (IMD)	IMD
8	Temperature	Gridded 1 degree data of India Meteorological Department (IMD)	IMD
9	Leaf Area Index	The MCD15A3H Version 6.1 of Moderate Resolution Imaging Spectroradiometer (MODIS) 4-day composite data at 500 m resolution	GEE
10	Streamflow	Daily gauged data observed by Central Water Commission (CWC)	India-WRIS
11	Groundwater level	Seasonal groundwater levels measured by Central Groundwater Board (CGWB)	India-WRIS

4.1.2 Time-series data

Time series data in WISDOM includes daily precipitation, daily temperature and 4-day composite Leaf Area Index (LAI). Like thematic layers, the time-series data can also be retrieved directly from GEE or IMD. The time-series data sets are pre-processed in WISDOM to remove data gaps and aggregate over the model grids. The observations, such as streamflow and groundwater level are used externally for validating the model results.

4.1.3 Model parameters

Various soil, land cover and aquifer parameters are required to run the integrated hydrologic model. The soil parameters include field capacity, wilting point, soil hydrologic group and saturated hydraulic conductivity. The land cover parameters include Curve Number (CN) and maximum root depth for each land cover class. Aquifer parameters include aquifer hydraulic conductivity, storage coefficients. Theses parameters are read from text files in WISDOM. Some of these parameters are tuned during model calibration.

4.1.4 Aquifer geometry

In the present case study, two aquifers are considered – the top unconfined aquifer and a confined aquifer following the NAQUIM reports. To model this two-aquifer system, three subsurface layers are defined, including an unconfined aquifer, an aquiclude layer and a confined aquifer layer. Thickness of these layers are defined by interpolating the NAQUIM data. The derived aquifer system is shown in the fence diagram in Figure 4.1.

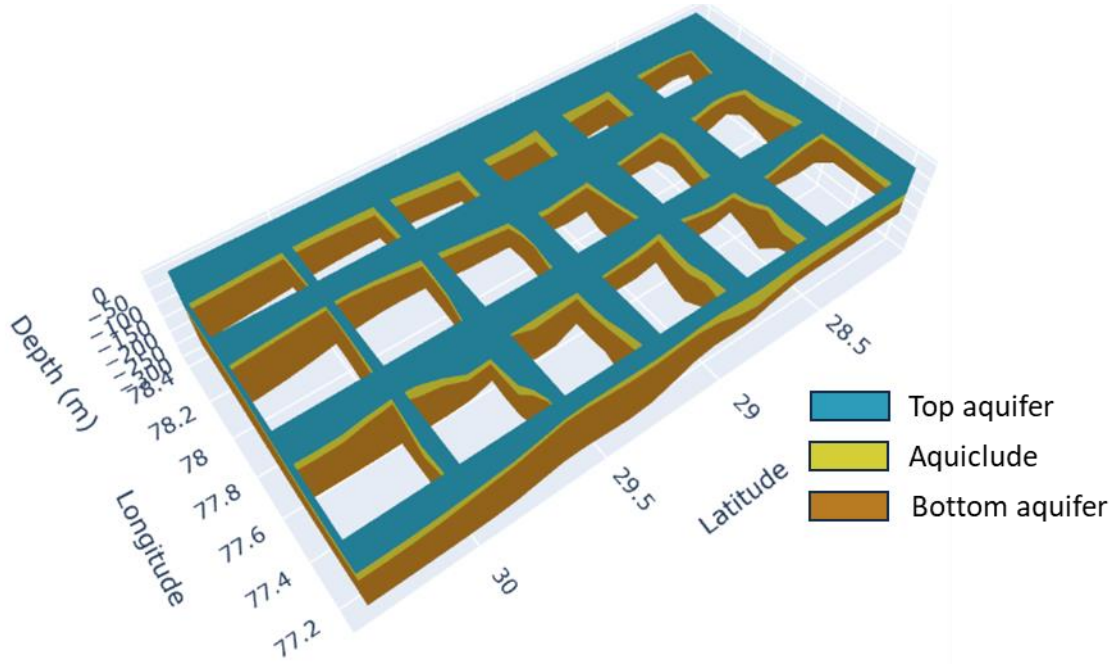

Figure 4.1. Fence diagram showing the derived aquifers from the interpolated point data

4.1.4 Boundary conditions

Boundary conditions are essential for simulating groundwater flow using groundwater model. WISDOM allows definition of all essential boundary conditions needed for groundwater flow modelling, including river, time-varying constant head, general head and well. The evapotranspiration and recharge are simulated using the UZF module and thus no additional

evapotranspiration and recharge boundary conditions are needed. For GYD, the river, well and constant head boundary conditions were defined. The location of these boundary conditions is shown in Figure 4.2. The river boundary includes the river Yamuna in the West and river Ganga in the West. The constant head boundary condition is applied in the Southern parts using observed groundwater heads. The pumping wells are derived automatically in WISDOM using pumping requirement and applied to each corresponding grid and this not shown in the map.

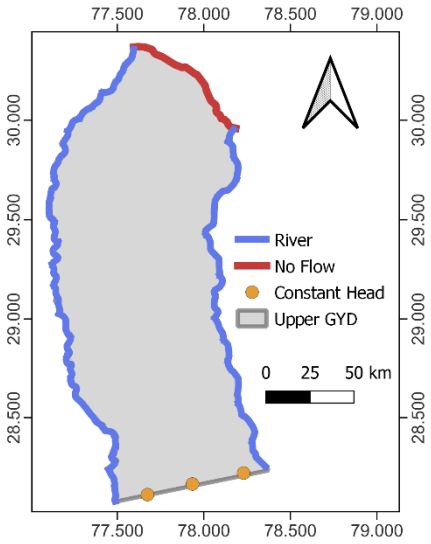

Figure 4.2. Boundary conditions - River, No Flow and Time-varying Constant Head - assigned for groundwater flow modelling

4.2 Model calibration and validation

The integrated modelling requires soil, land cover and aquifer parameters to be calibrated for reliable model outputs. Being closely coupled, the model has to be run in integrated mode with all the surface and subsurface models which necessitate calibration of both the surface and groundwater model simultaneously. A two-step calibration approach is used in this study. In the first step, the parameters are tuned manually by comparing groundwater head. In step two, the Parameter Estimation Program (PEST) was run to auto calibrate the model parameters. The large variations in parameters are done in the manual calibration whereas in the autocalibration the manually calibrated parameters are fine tuned further. The combination of manual and auto-calibration reduced the number of iterations for calibration. The initial parameter values with their optimized values are shown in the Table.

Table 4.2. Land cover parameters used in WISDOM. The calibrated values are shown in parenthesis.

Land cover	Amin	Amax	Bmin	Bmax	Cmin	Cmax	Dmin	Dmax	Maximum Root Depth (mm)
Bare	77	77	86	86	91	91	94	94	0
Shrubs	30	48	48	67	65	77	73	83	1800
Agriculture	**70 (68)**	**77 (75)**	**85 (75)**	**95 (85)**	**88 (83)**	**92 (88)**	**88 (86)**	**92 (90)**	**700 (1500)**
Urban	72	98	82	98	87	98	89	98	0

Forest	30	45	55	66	70	77	77	83	2300

Table 4.3. Soil parameters used in model. The calibrated values are shown in parenthesis.

Class	soil Hydrologic Group	Field Capacity	wilting Point	Soil moisture at saturatation	Ksat (m/d)
Sandy	A	0.08	0.03	0.43	9.22
loamy sand	A	0.15	0.06	0.42	2.61
sandy loam	A	0.21	0.09	0.4	1.26
Silty loam	B	0.32	0.12	0.46	0.95
Silt	B	0.28	0.08	0.52	2.06
Loamy	**B**	**0.29 (0.27)**	**0.14 (0.12)**	**0.43 (0.44)**	**0.47 (0.52)**
Sandy clay loam	C	0.27	0.17	0.39	0.58
Silty clay loam	D	0.36	0.21	0.48	1.1
Clay loam	**D**	**0.34 (0.32)**	**0.21 (0.18)**	**0.46 (0.48)**	**0.42 (0.38)**
Sandy clay	D	0.31	0.23	0.41	0.29
Silty clay	D	0.37	0.25	0.49	0.71
Clayey	D	0.36	0.27	0.47	0.76
other	B	0.36	0.27	0.47	0.76

Table 4.4. Aquifer parameters used in model. The calibrated values are shown in parenthesis.

Aquifer type	Hydraulic conductivity (m/d)	Sp. Yield	Sp. Storage
Sandstone or conglomerate	0.1 (0.08)	0.02 (0.05)	0.0005
Older alluvium	1 (4)	0.01 (0.07)	1.22E-04
Pebble/Gravel	5 (0.4)	0.05 (0.05)	0.0005
Younger alluvium	2 (1.6)	0.01 (0.05)	2.39E-05

4.2.1 Groundwater head

The observed groundwater head is compared with the simulated heads at different locations in the study area. The calibration was done for the period of 2011-13 and validation for the period of 2014-18. Figure 4.3 shows the comparison of groundwater heads for all locations at four different time-steps, viz. Jan 2011, July 2013, July 2015 and Jan 2018. A satisfactory performance is observed with R^2 of 0.98, 0.62, 0.74 and 0.87 during 2011, 2013, 2015 and 2018, respectively. The good agreement between the observed and simulated heads at these time steps indicate that the spatial pattern is reasonably captured by the model implies that the model simulated groundwater heads are useful for assessing spatial patterns at seasonal and annual scales.

The time-series of simulated head is compared with the observed heads at four different locations, namely Sakoti Tanda, Chota Mawana, Hapur and Lakhaothi (Figure 4.4). The

observed simulated heads were available at seasonal scale while the simulation is done at daily time step. The Root Mean Square Error (RMSE) varies considerably at each observation well indicating spatially inconstant model performance. The lowest RMSE (0.82) is observed at Chhota Mawana while the highest RMSE (4.23) is observed at Lahoathi. It is observed that the simulated heads deviate severely from the observed heads at some locations (such as Lakhaothi), specially during the later period (say after 2015). These discrepancies indicates that the model outputs with currently available data sets does not provide reliable results at daily/monthly time-steps, although, the results at annual scale and the spatial maps could still be useful for various impact assessments. The coarse scale aquifer data, such as aquifer thickness and storage coefficient, could be the main reason behind such poor model performance. Another key limitation has been the availability of observed groundwater levels. To develop a plausible model, observation data at a higher resolution (monthly) with a distributed observation network would be needed. The model performance must be improved with such detailed data in future for improved accuracy.

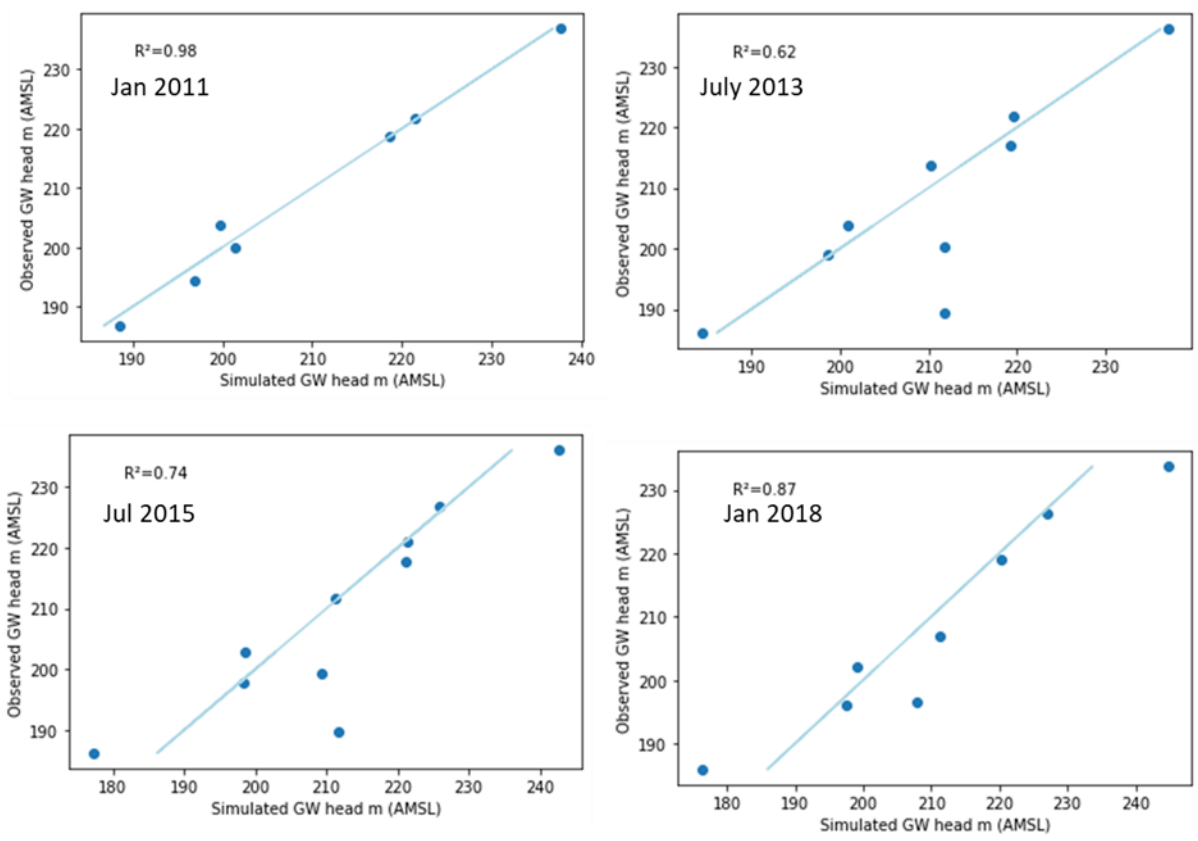

Figure 4.3. Comparison of simulated and observed groundwater head at different time-steps

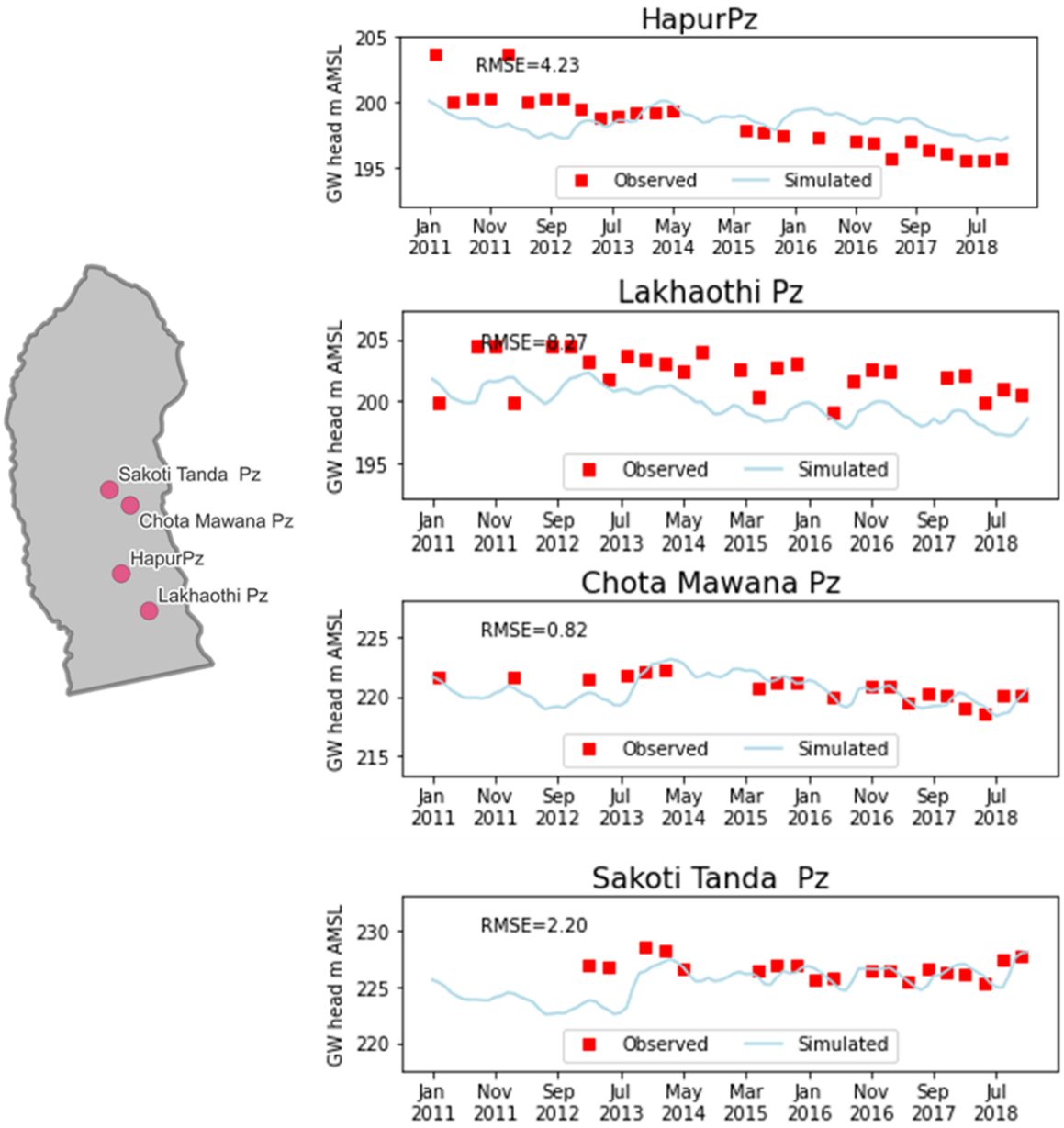

Figure 4.4. Comparison of groundwater head time-series at different locations

4.2.2 Groundwater recharge

The simulated groundwater recharge is compared with the recharge assessments of CGWB (Figure 4.5). CGWB assesses block-wise recharge using Groundwater Estimation Committee (GEC) norms (GEC, 2017). The GEC method uses the water table fluctuations and rainfall factor to estimate recharge. In this study, the district-wise recharge estimates of the year 2012 and 2016 are used for validating the recharge outputs of WISDOM. The grid-wise recharge of WISDOM is aggregated to districts level for comparison. The simulated recharge reasonably matches with CGWB's assessments. A high difference in recharge is observed for some districts, such as Meerut and Baghpat. It is also seen that the recharge matches more closely for the year 2012 as compared to 2016.

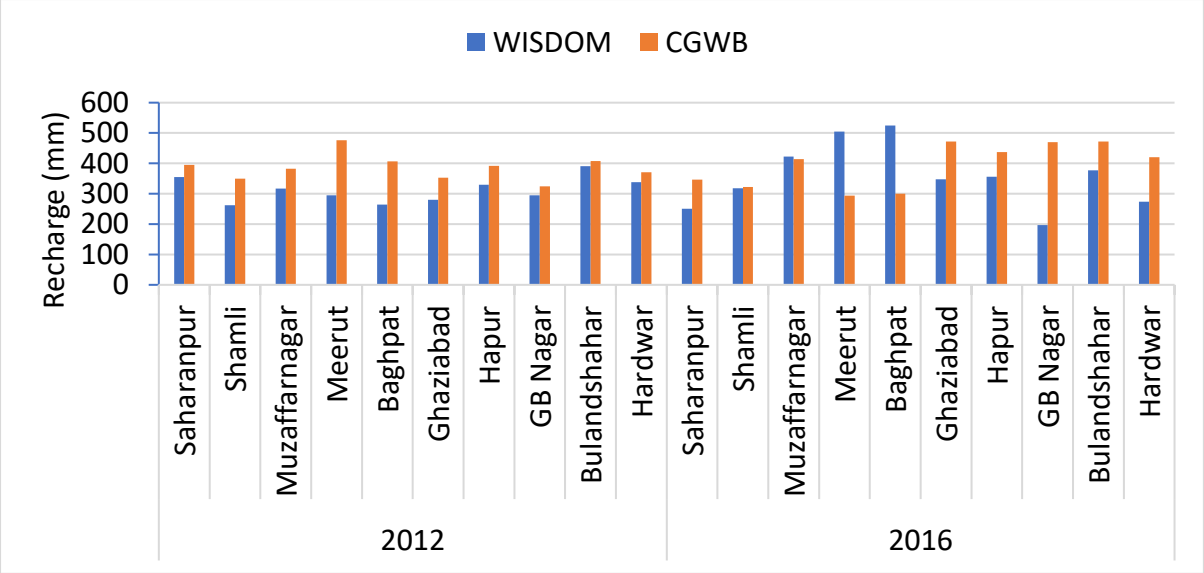

Figure 4.5. Comparison of recharge simulated by WISDOM and assessment of CGWB in the year 2012 and 2016

4.3 Model results

Being integrated, the WISDOM simulates various hydrologic processes in the soil root zone, unsaturated zone and groundwater zone. The model produces various hydrologic variables, such as runoff, streamflow, evapotranspiration, irrigation, groundwater extraction, recharge, groundwater flow, vadose zone soil moisture, etc. In addition, various thematic and time-series data are retrieved automatically during the model run, such as LAI, Potential Evapotranspiration (PET), vegetation fraction, etc. Some of the important model outputs are discussed in the following section.

4.3.1 Water budget

The simulated runoff, ET, recharge and field irrigation requirement for the period 2011 to 2018 is shown in Figure 4.6. The values shown in this figure is the average of all model grids in the respective years. In the study area, the ET is a major component of water budget which ranges from 737 to 823 mm. A considerable irrigation is applied in the area, ranging from 509 to 638 mm per year, leading to additional soil moisture for evapotranspiration. The runoff ranges from 98 to 247 mm per year. The groundwater recharge also varies considerably during the period, it varies from 217 to 425 mm. The water budget of the study area shows that the irrigation has a considerable contribution in recharge to groundwater in the study area.

4.3.2 Recharge to groundwater

Recharge is observed in the range of 20 to 40% of precipitation in the study area which exhibits considerable spatial and temporal variations. The annual recharge maps generated in WISDOM shows high recharge in the agricultural fields in the Northern parts near the Terai region (Figure 4.7). The higher precipitation in combination with irrigation during non-monsoon season might be leading to high recharge in these areas. The Southern portions generally receive lower precipitation leading to a lower recharge, however in some years, such as 2016, high recharge is observed due to high precipitation. It is observed that for few grids the model produces zero

recharge. These grids are mainly in the areas where the ET is very high and their entire soil moisture is consumed to meet transpiration needs and there is no moisture left for percolation. However, output of such grids should be modified in future with some addition field observations. The time-series of recharge at three different locations in the study area is also shown in Figure 4.8.

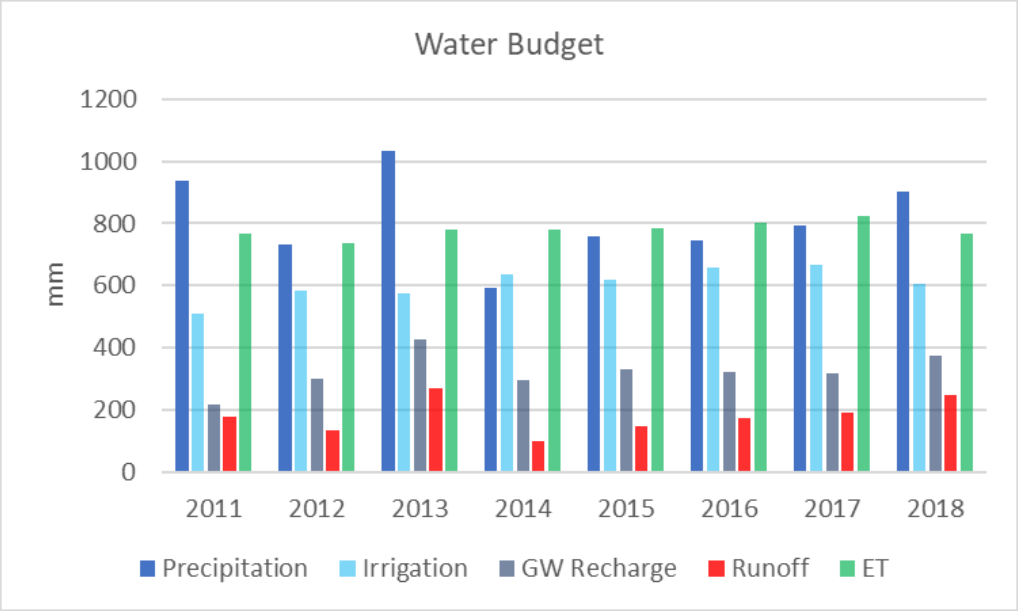

Figure 4.6. Water budget for the period 2011-18

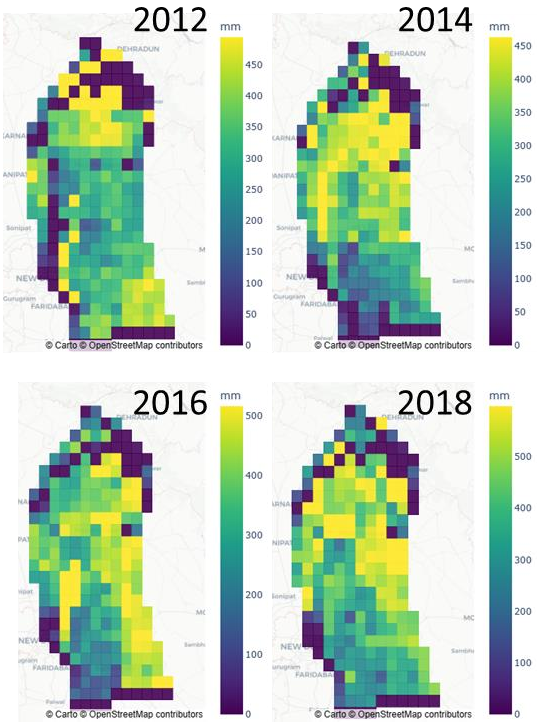

Figure 4.7. Annual groundwater recharge maps for the year 2012, 2014, 2016 and 2018.

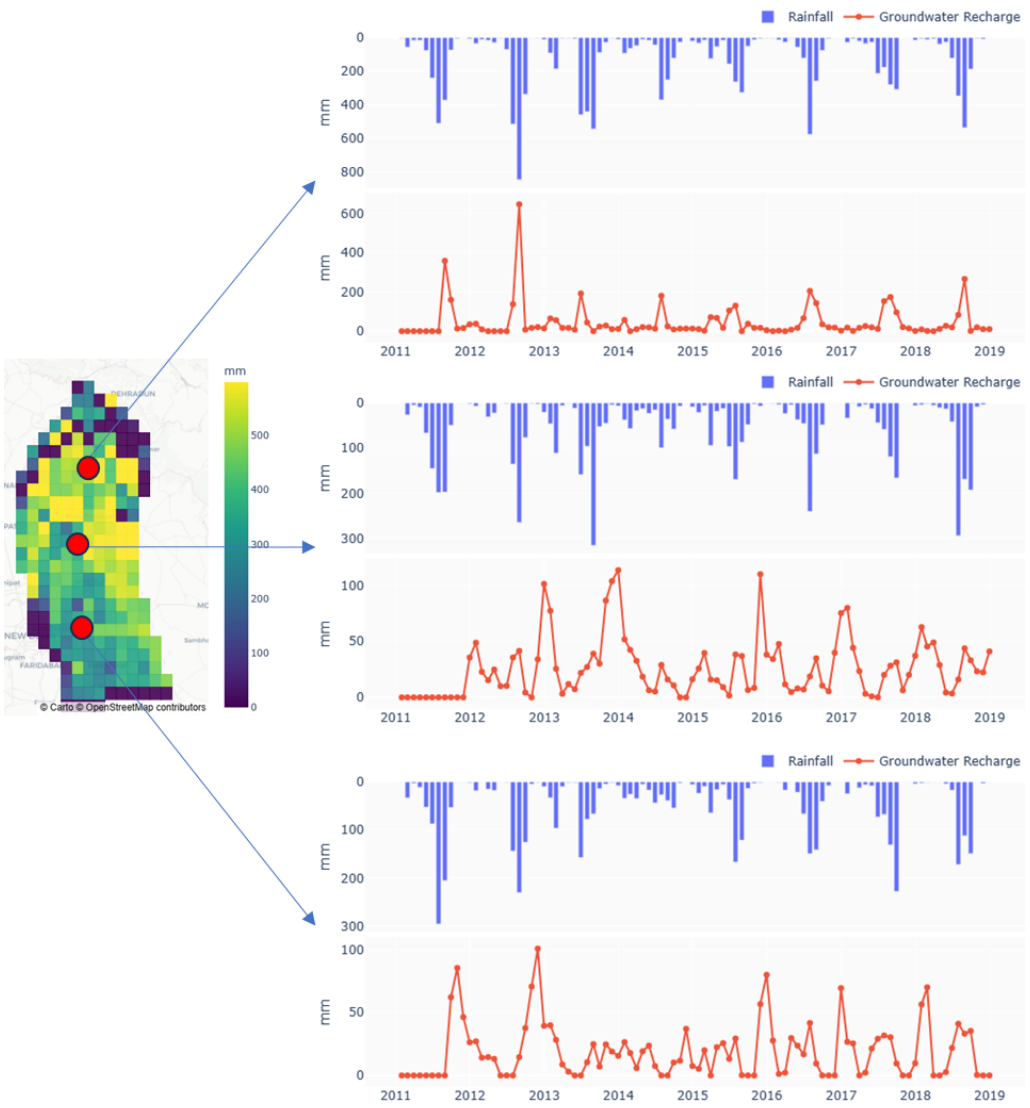

Figure 4.8. Monthly time-series of groundwater recharge at three different locations for the period 2011-18.

4.3.3 Irrigation requirement

Irrigation is one of the key governing factors for ET and recharge estimation. Since no consistent monthly/seasonal irrigation data is available for study region, we simulated the grid-wise irrigation requirement using WISDOM. The irrigation requirement is mainly governed by the LAI and precipitation in the region. The advantage of simulating the irrigation requirement in WISDOM is that the grid-wise pumping can also be estimated using irrigation and groundwater utilization fractions. The total irrigation demand is estimated and the fraction of total demand which is met from groundwater is calculated. Finally, the calculated groundwater extraction is converted to daily pumping and applied as well boundary condition in the model. The estimated irrigation, LAI and precipitation for Jun 2017 to May 2018 are shown in Figure 4.9. The irrigation demand is high when the LAI is high and precipitation is low, such as during the period from February to June. During the monsoon season, irrigation demand is low despite high LAI as the moisture deficit is replenished by precipitation during this season.

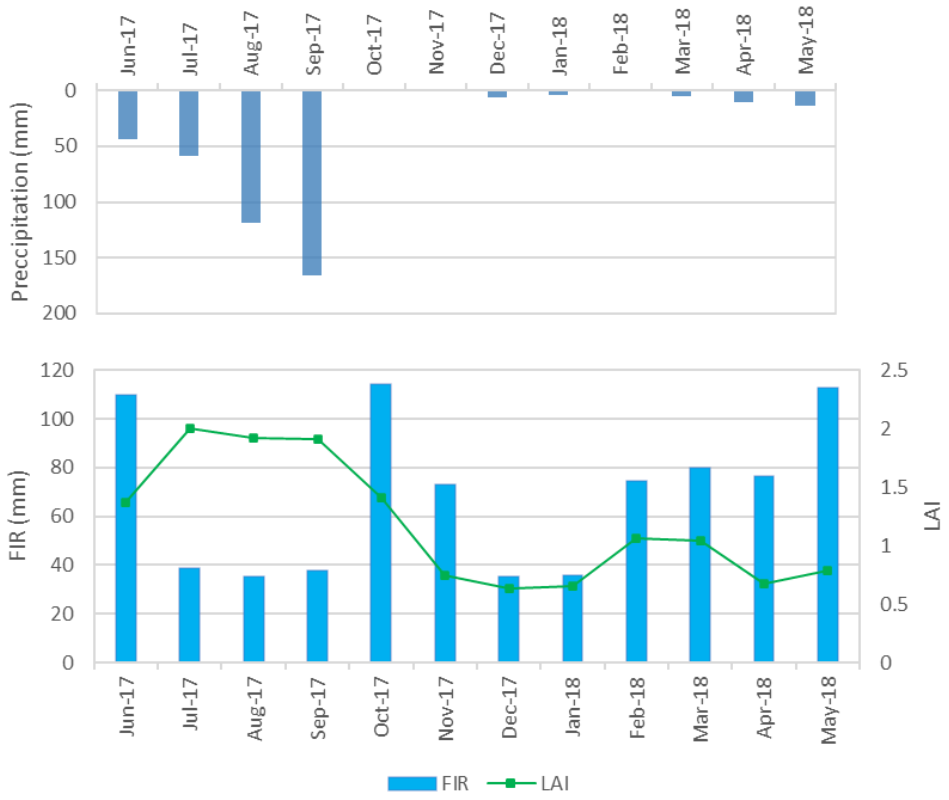

Figure 4.9. Monthly irrigation demand, LAI and precipitation for the period June 2017 to May 2018.

4.3.4 Vadose zone soil moisture

The soil moisture content and movement in the vadose zone is sometimes used as an indicator for validating the recharge to groundwater. The WISDOM simulates root zone soil moisture using RZF module and unsaturated zone soil moisture using MODLFOW's UZF module. WISDOM allows visualization of the soil moisture in the form of 3D Fence diagrams. Soil moisture up to a depth of 3 m for May 2018, August 2018 and December 2018 is shown in the Figure 4.10. The soil is observed to be dry (~0.15) during May 2018, which eventually get moisture during August due to monsoon. During the post monsoon the soil again starts getting dried due moisture extraction for transpiration by the plants.

4.4 Streamflow simulation in Upper Mahanadi Basin (UMB)

The WISDOM simulates streamflow using the integrated surface-groundwater model. The surface runoff is simulated using RZF and the baseflow is simulated using MODFLOW. The grid-based runoff is then routed to the basin outlet using MODFLOW's SFR module. To generate inputs, such as river grids, hydraulic connections between the grids and river geometry, the WISDOM encompasses an algorithm that derives these inputs using remote sensing data. Since the streamflow data was not available in GYD, the models are tested in upper Mahanadi basin up to Basantpur.

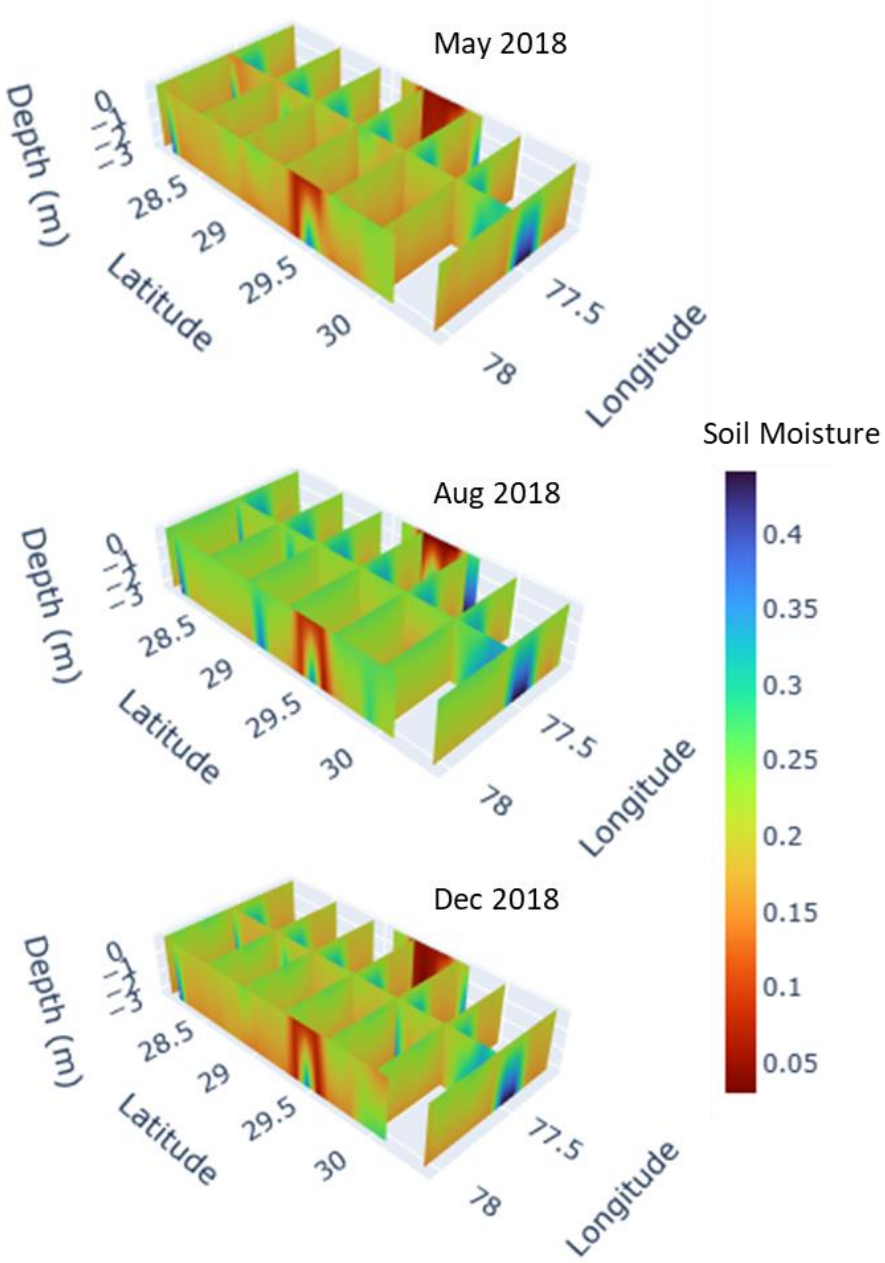

Figure 4.10 Vadose zone soil moisture for May, august and December 2018.

4.4.1 Model setup

Utilizing the automated data retrieval module of WISDOM, various time-series and thematic data which are available on GEE were downloaded. The key inputs used are, IMD's precipitation and temperature data, Copernicus 100 m land cover, SRTM 90 m DEM, soil texture map of NBSSS and LUP. The observed streamflow data of CWC was used for model validation. Since the objective was to test the streamflow simulation capability of WISDOM, a simplified groundwater model was developed using CGWB's aquifer data, such as aquifer thickness, storage coefficient and hydraulic conductivity.

The model was setup at 5 km spatial resolution and daily time-step. The *Basantpur*, a gauging station upstream of Hirakund dam, is selected as the basin outlet for the WISDOM. The simulation run was performed for the period 2001 to 2005.

4.4.2 Water budget

The precipitation varies from 974 to 1624 mm in the UMB during 2001-05 (Figure 4.11). The ET is the most dominating water budget component varying between 605 to 665 mm which is around 50% of precipitation. The recharge varies from 188 to 476 mm during the study period. Runoff has the lowers fraction of precipitation which varies between 82 to 206 mm. It may be noted that, in this case study, the irrigation was not considered and thus the results shown indicates the water budget under virgin catchment conditions. However, it still serves the purpose of validating the river routing capability of the WISDOM. The irrigation must be considered in future study for realistic recharge estimates.

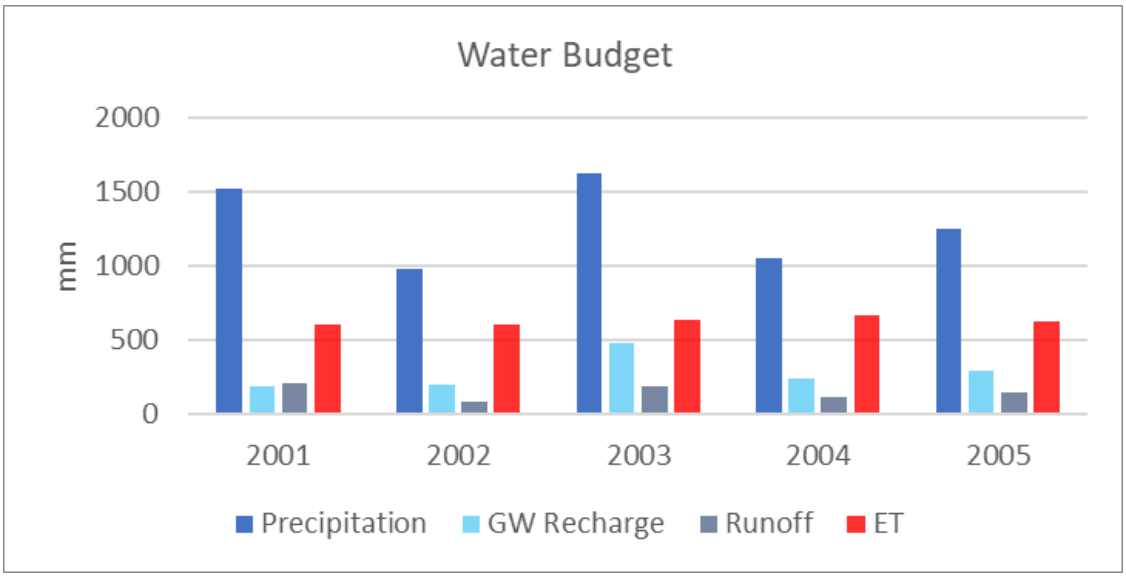

Figure 4.11. Water budget in the upper Mahanadi basin during 2001-05

4.4.3 Validation of streamflow

The streamflow simulated by WISDOM is compared with the observed streamflow at Basantpur. The model satisfactorily simulates streamflow at monthly time-scale with Nash-sutcliffe Efficiency (NSE) of 0.6 (Figure 4.12). It is found that for the year of normal precipitation, such as 2003 and 2005, the simulation of peak flows is better than that is in the higher or lower precipitation years, such as 2001 and 2002. Discrepancies in the initial period, such as in the year 2001, may be due inappropriate initial conditions and should be ignore considering 2001 as a spin-up period. During low precipitation in 2002, the influence of upstream reservoirs is prominent, leading to an overestimation.

The SFR used in WISDOM for streamflow routing is a steady-state routing model which assumes that all the overland flow generated on a day reaches to the outlet on the same day. The travel time and the resulted time-lag at the outlet has not been considered in SFR. This causes an early arrival of peak in the simulated flow, as can be seen in 2001, 2002 and 2005. This limitation of MODFLOW's SFR implies that the routed runoff should not be used

for flood assessment or stream flow simulation at event/sub-daily basis. However, for baseflow and streamflow simulation at a coarser scale, such as monthly/seasonal, could still be useful.

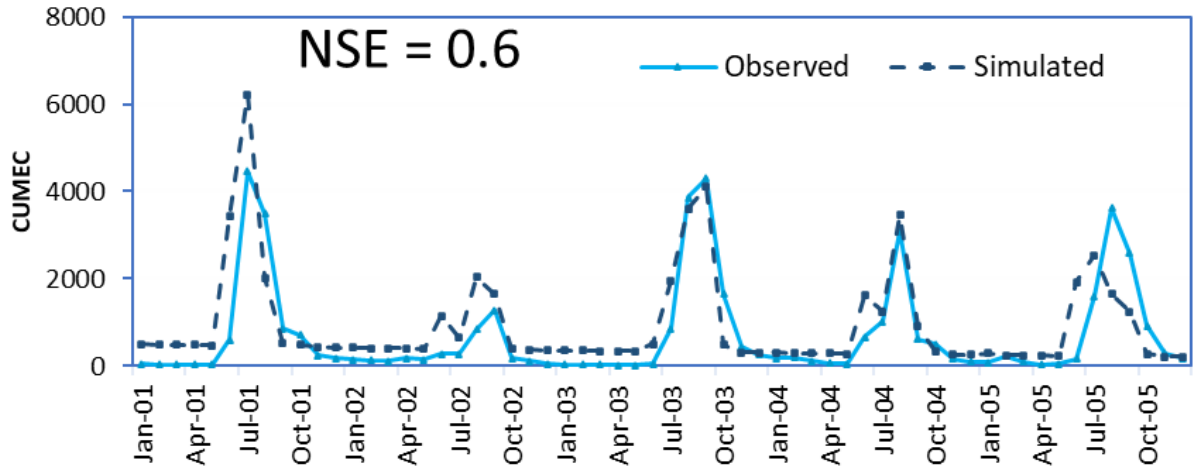

Figure 4.12 Monthly streamflow (observed vs. simulated) at Basantpur during 2001-05

***

Chapter-5

SCENARIO ANALYSIS

Groundwater is primary source of water for domestic and agricultural uses in many regions where perennial supply of surface water through rivers and canals is not available. Under perturbed hydrologic balance caused by anthropogenic and natural factors, the groundwater reservoirs serve as cushion and ensure persistent water supply. Therefore, it is important to assess future status of groundwater under various recharge and pumping scenarios. In this study, we formulated six scenarios of varying groundwater recharge and pumping and assessed the impacts on groundwater levels.

5.1 Description of scenarios

Six scenarios of groundwater recharge and extraction were formulated by perturbing the BAU recharge and extractions. Three scenarios of increased recharge, by 10, 20 and 30%, were prepared. Similarly, two scenarios of increased groundwater extraction by 20 and 40% were prepared.

Table 5.1. Description of groundwater recharge and extraction scenarios

Sr. No.	Scenario	Description
1	BAU	Business as Usual (BAU) groundwater recharge and extraction
2	RCH-10	Recharge increased by 10%
3	RCH-20	Recharge increased by 20%
4	RCH-30	Recharge increased by 30%
5	EXT-20	Groundwater extraction increased by 20%
6	EXT-40	Groundwater extraction increased by 40%

5.2 Estimation of groundwater extraction under BAU

In WISDOM, groundwater extraction is estimated utilizing the irrigation demand and groundwater utilization fraction. The irrigation demand is estimated using RZF module of WISDOM which simulates irrigation requirement using daily soil moisture deficit. It is assumed that the irrigation demand is met from surface and groundwater conjunctively. In many parts of GYD, supply from canal is available, therefore it is important to subtract the amount of demand being met from canal from the total irrigation demand so that the groundwater extraction can be worked out. CGWB provides district-wise fraction of demand that is met from groundwater (Figure 5.1). This groundwater utilization fraction file is used in model to estimate groundwater extraction. Based on daily irrigation demand and groundwater utilization fraction, total grid-wise groundwater pumping is estimated.

$$\text{GW extraction} = \text{irr. Demand} \times (1 - \text{Frac. of area irr. by canal}) \quad \textbf{(5.1)}$$

$$\text{Total supply} = \text{supply from canal} + \text{supply from GW} \quad \textbf{(5.2)}$$

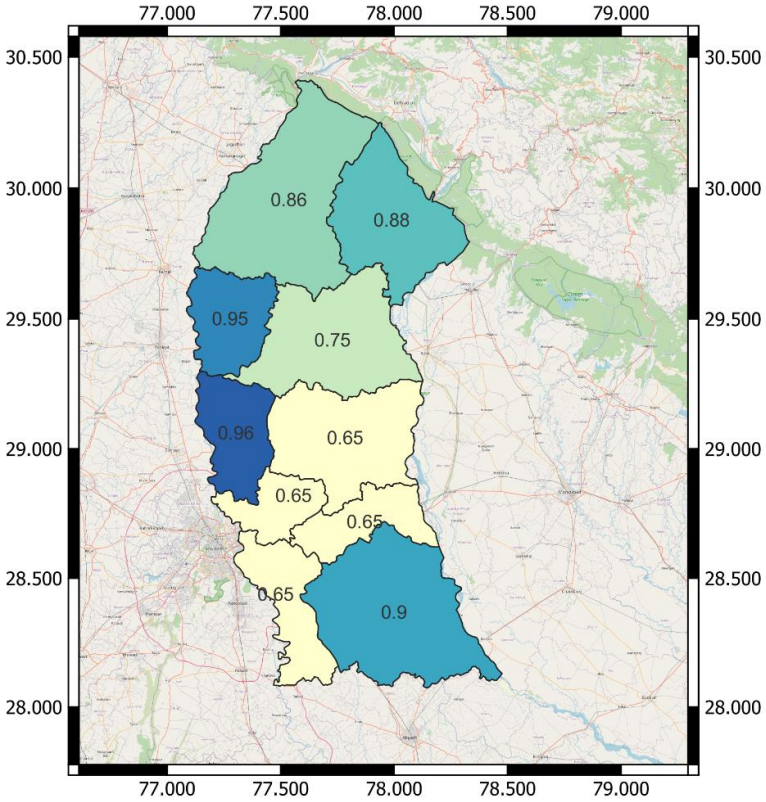

Figure 5.1. District-wise groundwater utilization fraction

5.3 Model run for scenario analysis

To analyse the recharge and extraction scenarios, the integrated model was run iteratively with different recharge/extraction inputs. Since both the recharge and groundwater pumping are estimated internally by the model, modification to the model scripts was required. To formulate the recharge scenarios, the RZF script is slightly modified to increase the recharge by 10, 20 and 30%. Similarly, the increased groundwater pumping, by 20 and 40%, is incorporated by modifying the pumping estimation module of RZF. Under both the modifications, the recharge/extraction is increased by the required fraction by multiplying the BAU recharge/extraction by respective factors.

5.4 Impacts of increased recharge

In the GYD, the average annual recharge to groundwater is estimated as 312 mm under BAU scenario. The recharge is increased to 343.2, 374.4 and 405.6 mm under RCH-10, RCH-20 and RCH-30 scenarios, respectively (Figure 5.2). The spatial maps of recharge under different scenarios are shown in Figure 5.3. Under the BAU scenario, the recharge is high in the central portion, varies from 500 to 800 mm from West to East, while the Northern and South-western parts have lower recharge. With 10% increase in recharge, the recharge increases further in the central and South-eastern parts. Similarly, under scenarios of increased recharge of 20 and 30% increase, recharge increases proportionately.

To assess the effect of increased recharge on groundwater levels, the depth to groundwater is mapped and shown in Figure 5.4. Under BAU Scenario, depth to groundwater is shallow near the rivers and towards the North-eastern part. A patch of deep groundwater is observed in the centre towards West where depth to groundwater is observed up to ~25 m. Under the scenarios of increased recharge, a considerable improvement in depth to groundwater is observed. The aquifer starts recovery when recharge is increased by 10%. With 20% increase in recharge, a considerable improvement in the groundwater levels is observed and the areas of overexploited groundwater improves considerably. Under the scenarios of 30% increase in recharge, the depleted groundwater recovers completely, however, in the areas of shallow groundwater, the groundwater rises near the ground surface which might lead to water-logging in these areas. Scenario of 20% increased recharge seems to be the most suitable scenario for the study area.

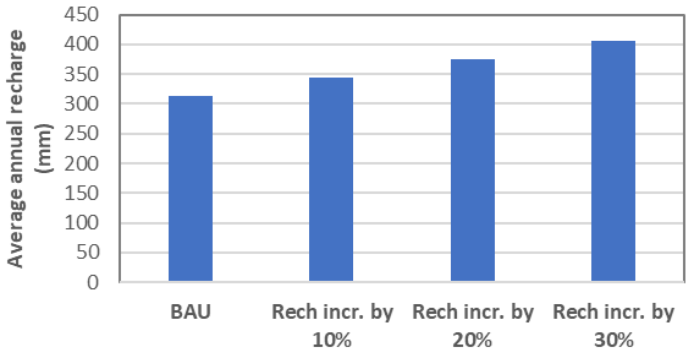

Figure 5.2. Groundwater recharge under BAU and increased recharge scenarios

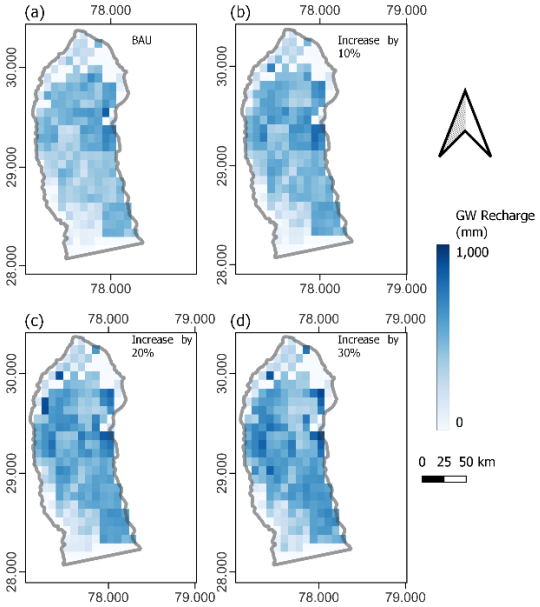

Figure 5.3 Groundwater recharge maps under BAU (a) and scenarios of increased recharge by 10, 20 and 30% (b, c and d, respectively)

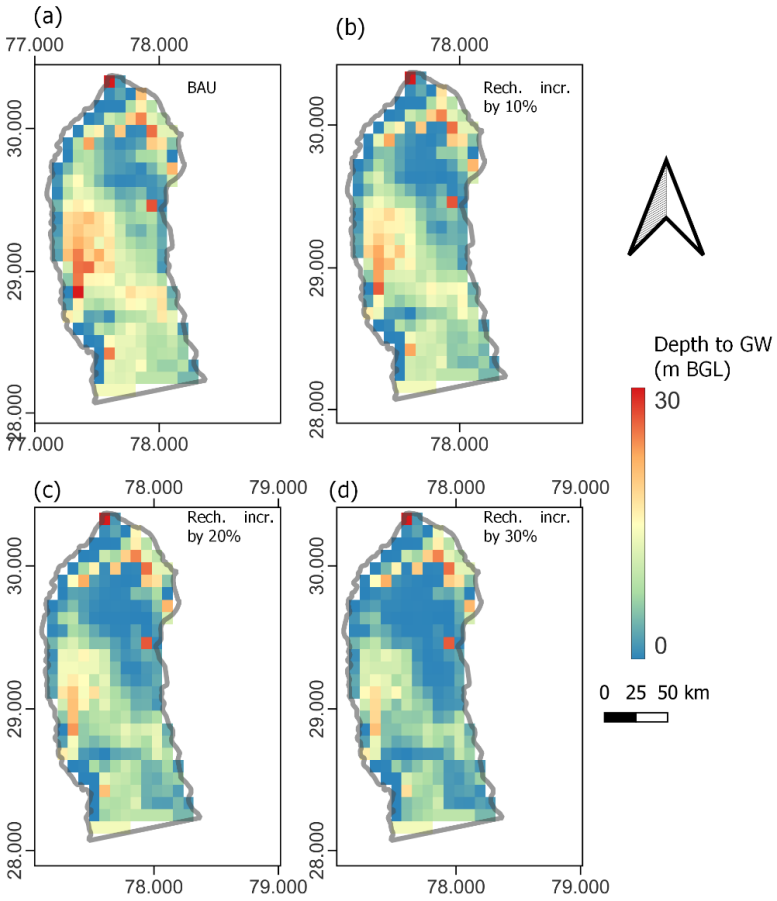

Figure 5.4 Depth to groundwater under BAU (a) and scenarios of increased recharge by 10, 20 and 30% (b, c and d, respectively)

5.5 Impacts of increased pumping

Assessment of the impacts of groundwater extraction on groundwater levels is assessed by creating scenarios of increased groundwater extraction by 20% and 40%. In the GYD, the average annual groundwater extraction is estimated as 9557 MCM under BAU scenario. The extraction is increased to 11469 and 13033 MCM under EXT-20 (increase by 20%) and EXT-40 (increase by 40%) scenarios, respectively (Figure 5.5).

To assess the effect of increased pumping on groundwater levels, the depth to groundwater is mapped and shown in Figure 5.6. Under BAU Scenario, depth to groundwater is shallow near the rivers and towards the North-eastern part. A patch of deep groundwater is observed in the centre towards West where depth to groundwater is observed up to ~25 m. Under the scenarios of increased pumping, a considerable decline in depth to groundwater is observed. The aquifer starts depleting when pumping is increased by 20%. With 40% increase in pumping, a considerable depletion in groundwater is observed and the central area becomes overexploited with depth to groundwater up to 45 m. The scenarios of increased groundwater pumping/extraction indicates that if such increase in pumping occurs, the groundwater system of GYD might fail to supply water in many parts of the basin. In addition, such increase in pumping might lead to poor groundwater quality and reduced baseflow contribution to rives.

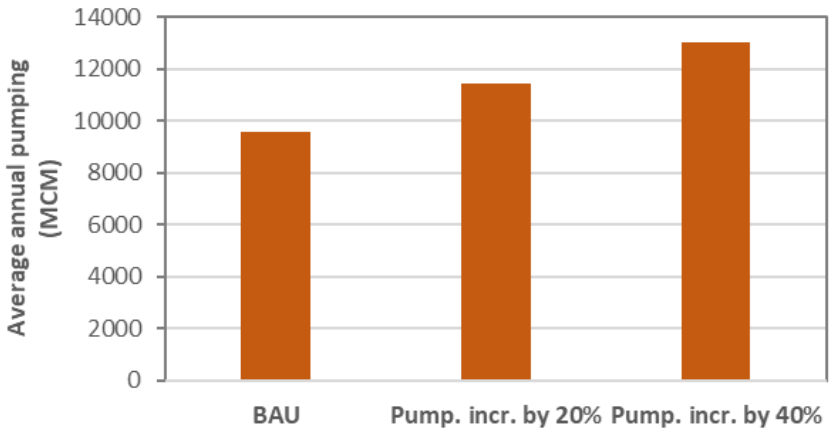

Figure 5.5. Groundwater extraction under BAU and increased pumping scenarios

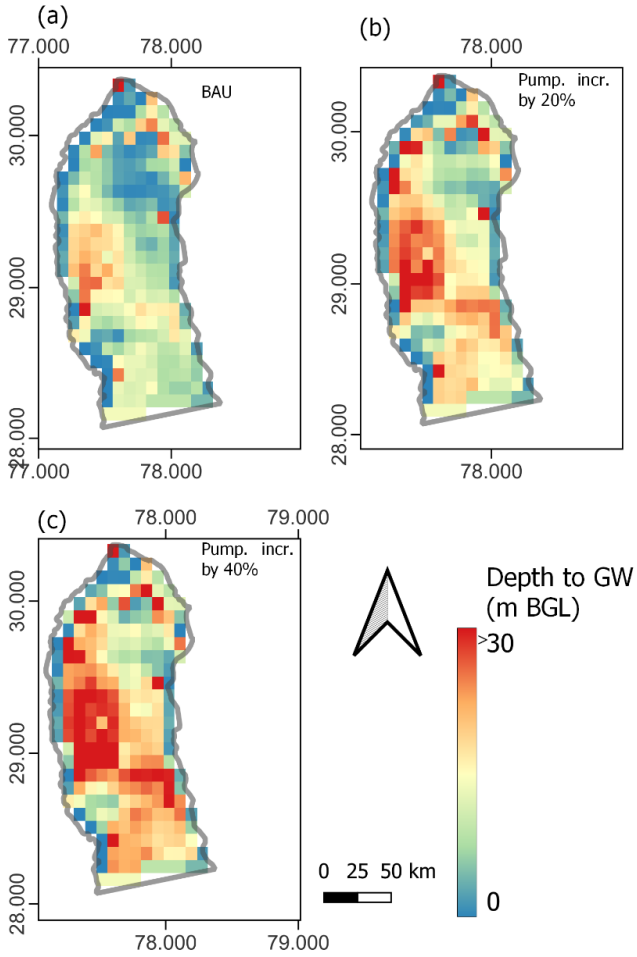

Figure 5.6 Depth to groundwater under BAU (a) and scenarios of increased pumping by 20, 40% (b and c, respectively)

***

Chapter-5

CONCLUDING REMARKS

General

Hydrologic modelling is valuable to support decision making for forming water management strategies to ensure water availability. To enhance the capabilities of hydrologic models, an integrated system is envisaged with cloud-computing, web-based interface and integrated models. In this light, a web-based system is developed and tested in this study. The current version of the system is developed mainly to estimate groundwater recharge, even though it can also simulate runoff, streamflow, ET and crop water demand/supply using standard methods. The developed system is tested in Hindon river basin and upper Mahanadi basin. The former application aims at validating the groundwater recharge, while the later aims at testing the streamflow simulation. To assign the boundary conditions appropriately in Hindon basin, the model domain is extended to river Yamuna in the West and river Ganga in the East and the extended area is referred as Ganga Yamuna Doab (GYD). The developed system is also used for creating hypothetical recharge/abstraction scenarios for assessing the impacts on groundwater system in GYD.

Development of system for integrated modelling

Estimation of recharge requires simulation of both the surface and subsurface hydrological processes as it is an end-result of various processes happening at surface and subsurface. Recharge is governed by various influxes, such as infiltration and irrigation, and outfluxes, such as root water uptake and soil evaporation. Therefore, in order to mimic all such processes, an integrated model is needed. The integrated model developed in this study consists of various modules which simulate processes in unsaturated and saturated zones. The model has three simulation modules, namely Root Zone Flow (RZF), Unsaturated Zone Flow (UZF), and Groundwater Flow (GWF). The integrated model is encapsulated into a web-based system which consists of python-based modules, Google Earth Engine (GEE) API, thematic and time-series database. The developed integrated system is named as NIH's **W**eb-based **I**ntegrated Catchment Modelling **S**ystem for **D**ecisi**o**n **M**aking (NIH-WISDOM). It is empowered by well-stablished hydrologic models, such as MODFLOW, for reliable hydrologic simulations. Thereby, it uses the emerging web and cloud-based techniques with the advantage of well-tested models for better reliability.

The RZF module is developed during the present study at NIH to simulate processes in the top soil layer (say, up to 500 mm). All the processes happening at the surface and top soil layer, such as runoff, infiltration, ET from top soil layer, soil evaporation, etc., are simulated by RZF. RZF is tightly coupled with Unsaturated Zone Flow (UZF) module to further simulate the processes in the vadose zone, such as ET from deep roots and recharge. Irrigation is an important influx to sub-surface system that considerably affect AET, soil moisture and recharge. Estimation of irrigation demand in the model is based on the soil moisture balance in the RZF. At each time-step, the available soil moisture is estimated and the irrigation is added

when soil moisture depletes beyond the specified allowable depletion. Groundwater pumping is an important component to estimate safe groundwater extraction and is also an input to MODFLOW. In WISDOM, the groundwater extraction is estimated internally utilizing the irrigation demand estimates. For estimation of baseflow/river seepage and calibration/validation of integrated model, it is important to rout the runoff to the basin outlet / discharge gauging sites. The routing models require various inputs related to river geometry, segment lengths and hydraulic connectivity between reaches. Also, to route the overland flow to river, it is important to know watershed of each river reach and their connectivity. Creation of such inputs require considerable effort and time. In WISDOM, derivation of these river attributes is automated utilizing HydroShed and Global River Database. Runoff routing is done using the Surface Flow Routing (SFR) package of MODFLOW.

The UZF aims at simulating the flow in unsaturated zone. In case of WISDOM, the UZF simulates flow in the zone below the root zone (as simulated by RZF) but above the water table. UZF is a 1-D Richards Equation-based module of MODFLOW which is tightly coupled with RZF and GWF modules. The percolation from the top soil layer becomes the influx to the bottom soil layer which consists the deeper root and the unsaturated zone. Groundwater flow simulation is vital for simulation of recharge-pumping effects and river-aquifer interaction. WISDOM uses the very popular – modular hydrologic simulation program called MODFLOW – developed by U.S Geological Survey.

The WISDOM also encompasses GEE along with a data processing module for automated data retrieval and processing. A web-based interface is also developed to run the model using web-browser. The following are the key enhancement of WISDOM over traditional models (i) incorporation of the phenological variations in the model using 4-day composite Leaf Area Index, (ii) automated data retrieval and processing. (iii) provision to disseminate outputs to web-based platform so as to support decision making.

Validation of results

The observed groundwater head is compared with the simulated heads at different locations in the GYD during calibration (2011-13) and validation (2014-18). A satisfactory performance is observed with R^2 of 0.98, 0.62, 0.74 and 0.87 during 2011, 2013, 2015 and 2018, respectively. It is found that the spatial pattern is reasonably captured by model implies that the results are useful for assessing spatial patterns at seasonal and annual scales. The Root Mean Square Error (RMSE) varies considerably at each observation well indicating spatially inconstant model performance. The lowest RMSE (0.82) is observed at *Chhota Mawana* while the highest RMSE (4.23) is observed at *Lahoathi*. It is observed that the simulated heads deviate severely from the observed heads at some locations (such as *Lakhaothi*), specially during the later period (say after 2015). These discrepancies indicates that the model outputs with currently available data sets does not provide reliable results at daily/monthly time-steps, although, the results at annual scale and the spatial maps could still be useful for various impact assessments. The district-wise recharge estimates of CGWB for the year 2012 and 2016 are compared with model outputs in GYD. The simulated recharge reasonably matches with CGWB's assessments. A high difference in recharge is observed for some districts, such as *Meerut* and *Baghpat*. It is also seen that the recharge matches more closely for the year 2012 as compared to 2016.

The simulated streamflow is compared with the observed streamflow at Basantpur in upper Mahanadi basin. The model satisfactorily simulates streamflow at monthly time-scale with Nash-sutcliffe Efficiency (NSE) of 0.6. It is found that for the year of normal precipitation, such as 2003 and 2005, the simulation of peak flows is better than that is in the higher or lower precipitation years, such as 2001 and 2002.

Scenario analysis

Under perturbed hydrologic balance caused by anthropogenic and natural factors, the groundwater reservoirs serve as cushion and ensure persistent water supply. Therefore, it is important to assess future status of groundwater under various recharge and pumping scenarios. In this study, we formulated six scenarios of varying groundwater recharge and pumping and assessed the impacts on groundwater levels. The scenarios of groundwater recharge and extraction were formulated by perturbing the Business-as-Usual (BAU) recharge and extractions. Three scenarios of increased recharge, by 10, 20 and 30%, were prepared. Similarly, two scenarios of increased groundwater extraction by 20 and 40% were prepared.

In the GYD, the average annual recharge to groundwater is estimated as 312 mm under BAU scenario. The recharge is increased to 343.2, 374.4 and 405.6 mm under scenarios of 10, 20 and 30% increased recharge, respectively. Under BAU Scenario, depth to groundwater is shallow near the rivers and towards the North-eastern parts. A patch of deep groundwater is observed in the centre towards West with depth up to ~25 m. Under the scenarios of increased recharge, a considerable improvement in depth to groundwater is observed. The aquifer starts recovery when recharge is increased by 10%. With 20% increase in recharge, a considerable improvement in the groundwater levels is observed and the areas of overexploited groundwater improves considerably. Under the scenarios of 30% increase in recharge, the depleted groundwater recovers completely, however, in the areas of shallow groundwater, the groundwater rises near the ground surface which might lead to water-logging in these areas. Scenario of 20% increased recharge seems to be the most suitable scenario for the study area.

The average annual groundwater extraction is estimated as 9,557 MCM under BAU scenario. The extraction is increased to 11,469 and 13,033 MCM under the increased extraction by 20% and 40%, respectively. The aquifer starts depleting when pumping is increased by 20%. With 40% increase in pumping, a considerable depletion in groundwater is expected and the central area becomes overexploited with depth to groundwater up to 45 m. The analysis indicates that if such increase in pumping occurs, the groundwater system of GYD might fail to supply water in many parts of the basin. In addition, such increase in pumping might lead to poor groundwater quality and reduced baseflow contribution to rives.

Implications and limitations of the study

The NIH-WISDOM developed in this study utilizes hydrologic models and various open-source Python libraries. WISDOM provides effortless data retrieval and processing for integrated modelling. With its web-based interface, WISDOM allows interactive visualization of various thematic, time-series, and 3D data. The key advantages of using WISDOM are as follows:

I. WISDOM offers a web-based interface for model conceptualization, data preparation, and output visualization. All computations are performed on the server, eliminating the need for model installation and software configurations on a local computer. The model can be accessed and utilized through a web browser.

II. The integrated RZF-UZF-GWF simulation enables the estimation of river-aquifer interaction with routed runoff and baseflow at the basin outlet. WISDOM employs an automated algorithm for river grid delineation and input preparation, providing an efficient way to assign river parameters for MODFLOW's SFR module.

IV. The GEE plug-in allows automated data retrieval from the Earth Engine cloud, along with data pre-processing. Various time-series data, such as LAI and precipitation, and thematic data, including land cover, soil, elevation, and slope, can be directly retrieved from GEE.

V. Various Python scripts are developed and integrated into WISDOM to automate input file preparation for the simulation modules, streamlining the process of performing quick model runs.

During the testing of the developed system, some limitations are also noted.

I. The integrated model was tested for auto-calibration using Parameter Estimation Program (PEST) and it is found that the run time during parameter optimization is high at daily time-step. Therefore, an option to run the model at monthly time-step would be required for auto-calibration.

II. An algorithm is developed to derive hydraulic connections between river grids and generate inputs for SFR module of MODFLOW. The developed algorithm performs satisfactorily, however tuning of thresholds used in the algorithm is needed for deriving inputs for small rivers.

III. In the current version, all the models run in integration and inputs for all surface-subsurface models are needed. Options to run the models independently would be a useful feature.

Another constraint observed during the modelling is the limited data availability. The coarse scale aquifer data, such as aquifer thickness, storage coefficient and data for model calibration, affects model accuracy. To develop a plausible model, observed data at a higher frequency (monthly) with a distributed observation network would be needed. The model performance must be improved with such detailed data in future for improved accuracy.

The results of the scenario analysis indicate potential benefits of managed recharge, if implemented in future, for groundwater replenishment and groundwater sustainability. The increase in recharge by 10, 20 and 30% is applied uniformly to all model grids. Such uniform increase in recharge is only possible due to changes in precipitation due to climate variability. However, to obtain such increase in recharge using artificial recharge measures seems to be impossible as the recharge measures are generally implemented at few selected locations. Therefore, the resultant increase in recharge due to managed aquifer recharge is generally small and large-scale recharge projects might be needed to obtain notable improvements. Despite

these limitations, the results obtained in this study are useful in planning the recharge measures. The responses of groundwater system against the increased recharge and pumping still be useful for planning the managed aquifer recharge measures.

Scope for future studies

Development of NIH-WISDOM opens new opportunities for further enhancement in models and interface. Important modifications that would improve the model reliability and functionality are as follows:

I. Incorporation of surface hydrologic models, such as Variable Infiltration Capacity (VIC) model, will expand the applicability of the system for surface hydrologic modelling and will also improve results of integrated modelling.
II. The WISDOM simulates irrigation demand and supply at model grids. Provision to perform such estimates at canal commands will make it better for irrigation planning. Integration of a command-based system model with all demand components, such as irrigation, domestic and industrial demands, may improve the model functionality.
III. Improvement in various modules of WISDOM may be made to reduce computation time which will eventually improve the auto-calibration.

In the light of these limitations and scope as mentioned above, a study has been taken-up at NIH. The proposed study aims at incorporating VIC model, developing utility tools for trend analysis and map creation, and enhancing the existing modules of WISDOM.

***

REFERENCES

Abiye, T. (2016). Synthesis on groundwater recharge in Southern Africa: A supporting tool for groundwater users. *Groundwater for Sustainable Development*, *2–3*(October), 182–189. https://doi.org/10.1016/j.gsd.2016.10.002

Alam, S., Borthakur, A., Ravi, S., Gebremichael, M., & Mohanty, S. K. (2021). Managed aquifer recharge implementation criteria to achieve water sustainability. *Science of The Total Environment*, *768*, 144992. https://doi.org/10.1016/j.scitotenv.2021.144992

Andreadis, K. M., Schumann, G. J. P., & Pavelsky, T. (2013). A simple global river bankfull width and depth database. *Water Resources Research*, *49*(10), 7164–7168. https://doi.org/10.1002/wrcr.20440

Assefa, K. A., & Woodbury, A. D. (2013). Transient, spatially varied groundwater recharge modeling. *Water Resources Research*, *49*(8), 4593–4606. https://doi.org/10.1002/wrcr.20332

Bailey, R. T., Wible, T. C., Arabi, M., Records, R. M., & Ditty, J. (2016a). Assessing regional-scale spatio-temporal patterns of groundwater–surface water interactions using a coupled SWAT-MODFLOW model. *Hydrological Processes*, *30*(23), 4420–4433. https://doi.org/10.1002/hyp.10933

Bailey, R. T., Wible, T. C., Arabi, M., Records, R. M., & Ditty, J. (2016b). Assessing regional-scale spatio-temporal patterns of groundwater–surface water interactions using a coupled SWAT-MODFLOW model. *Hydrological Processes*, *30*(23), 4420–4433. https://doi.org/10.1002/hyp.10933

Batelaan, O., & DeSmedt, F. (2001). WetSpass: a flexible, GIS based, distributed recharge methodology for regional groundwater modelling. *Impact of Human Activity on Groundwater Dynamics*, *269*, 11–17.

Bay, C., Kang, H., & Sridhar, V. (2019). Drought assessment with a surface-groundwater coupled model in the Chesapeake Bay watershed. *Environmental Modelling & Software*, *119*, 379–389.

Boulain, N., Cappelaere, B., Séguis, L., Favreau, G., & Gignoux, J. (2009). Water balance and vegetation change in the Sahel: A case study at the watershed scale with an eco-hydrological model. *Journal of Arid Environments*, *73*(12), 1125–1135. https://doi.org/10.1016/j.jaridenv.2009.05.008

Cao, G., Scanlon, B. R., Han, D., & Zheng, C. (2016). Impacts of thickening unsaturated zone on groundwater recharge in the North China Plain. *Journal of Hydrology*, *537*, 260–270. https://doi.org/10.1016/j.jhydrol.2016.03.049

CGWB. (2020). *Master Plan for Artificial Recharge to Groundwater in India, Central Ground Water Board, Ministry of Jal Shakti, Government of India*.

CGWB. (2022). *National Compilation on Dynamic Ground Water Resources of India, 2022, Central Ground Water Board, Ministry of Jal Shakti, Government of India*.

Constance L Danner, Daene C McKinney, Rebecca Teasley, & Sandoval-Solis, S. (2006). *Documentation and Testing of the WEAP Model for the Rio Grande/Bravo Basin, Center for Research in Water Resources, Bureau of Engineering Research, the University of Texas at Austin*. http://www.ce.utexas.edu/centers/crwr/reports/online.html

CGWB. (2017). *Aquifer Mapping and Ground Water Management Plan, Central Groundwater Board, Ministry of Water Resources, River Development and Ganga Rejuvenation, Government of India*.

Evans, S. W., Jones, N. L., Williams, G. P., Ames, D. P., & Nelson, E. J. (2020). Groundwater Level Mapping Tool: An open source web application for assessing groundwater sustainability. *Environmental Modelling & Software*, *131*, 104782. https://doi.org/10.1016/j.envsoft.2020.104782

Gorelick, N., Hancher, M., Dixon, M., Ilyushchenko, S., Thau, D., & Moore, R. (2017). Google Earth Engine: Planetary-scale geospatial analysis for everyone. *Remote Sensing of Environment*, *202*, 18–27. https://doi.org/10.1016/j.rse.2017.06.031

Hamed, K. H., & Rao, A. R. (1998). A modified Mann-Kendall trend test for autocorrelated data. *Journal of Hydrology*, *204*, 196.

Imig, A., Szabó, Z., Halytsia, O., Vrachioli, M., Kleinert, V., & Rein, A. (2022). A review on risk assessment in managed aquifer recharge. *Integrated Environmental Assessment and Management*, *18*(6), 1513–1529. https://doi.org/10.1002/ieam.4584

Langevin, C. D., Hughes, J. D., Banta, E. R., Niswonger, R. G., Panday, S., & Provost, A. M. (2017). Documentation for the MODFLOW 6 Groundwater Flow Model: U.S. Geological Survey Techniques and Methods. In *USGS: Techniques and Methods 6-A55*. https://doi.org/https://doi.org/10.3133/tm6A55

Lehner, B., Verdin, K., & Jarvis, A. (2008). New global hydrography derived from spaceborne elevation data. *Eos*, *89*(10), 93–94. https://doi.org/10.1029/2008EO100001

Mountjoy Daniel, & Low Glen. (2017). A Groundwater Recharge Assessment Tool (GRAT). *GRA Conference*.

Mukherjee, A., Bhanja, S. N., & Wada, Y. (2018). Groundwater depletion causing reduction of baseflow triggering Ganges river summer drying. *Scientific Reports*, *8*(1), 12049. https://doi.org/10.1038/s41598-018-30246-7

Mutanga, O., & Kumar, L. (2019). Google Earth Engine Applications. *Remote Sensing*, *11*(5), 591. https://doi.org/10.3390/rs11050591

GEC. (2017). *Ground Water Resource Estimation Committee, Ministry of Water Resources, River Development & Ganga Rejuvenation, Government of India*.

Neitsch, S. L., Arnold, J. G., Kiniry, J. R., & Williams, J. R. (2011). *Soil and Water Assessment Tool: Theoretical Documentation-Version 2009*.

Niswonger, R. G., & Prudic, D. E. (2010). *Documentation of the Streamflow-Routing (SFR2) Package to Include Unsaturated Flow Beneath Streams-A Modification to SFR1 Section A, Ground Water, of Book 6, Modeling Techniques*. http://www.usgs.gov/

Niswonger, R. G., Prudic, D. E., & Regan, S. R. (2006). Documentation of the Unsaturated-Zone Flow (UZF1) Package for Modeling Unsaturated Flow Between the Land Surface and the Water Table with MODFLOW-2005. *U.S. Geological Survey Techniques and Methods*, 71.

Peng, H., Jia, Y., Tague, C., & Slaughter, P. (2015). An eco-hydrological model-based assessment of the impacts of soil and water conservation management in the Jinghe River Basin, China. *Water (Switzerland)*, *7*(11), 6301–6320. https://doi.org/10.3390/w7116301

Sallwey, J., Schlick, R., Bonilla Valverde, J. P., Junghanns, R., Vásquez López, F., & Stefan, C. (2019). Suitability Mapping for Managed Aquifer Recharge: Development of Web-Tools. *Water*, *11*(11), 2254. https://doi.org/10.3390/w11112254

Scanlon, B. R., Healy, R. W., & Cook, P. G. (2002). Choosing appropriate techniques for quantifying groundwater recharge. *Hydrogeology Journal*, *10*, 18–39. https://doi.org/Doi 10.1007/S10040-002-0200-1

Szabó, Z., Szijártó, M., Tóth, Á., & Mádl-Szőnyi, J. (2023). The Significance of Groundwater Table Inclination for Nature-Based Replenishment of Groundwater-Dependent Ecosystems by Managed Aquifer Recharge. *Water*, *15*(6), 1077. https://doi.org/10.3390/w15061077

Umar, R., Ahmed, I., Alam, F., & Khan, M. M. (2009). Hydrochemical characteristics and seasonal variations in groundwater quality of an alluvial aquifer in parts of Central Ganga Plain, Western Uttar Pradesh, India. *Environmental Geology*, *58*(6), 1295–1300. https://doi.org/10.1007/s00254-008-1630-4

USDA - SCS. (1972). Soil Conservation Service, National Engineering Handbook. Section 4, Hydrology. In *National Engineering Handbook*.

Vos, K., Splinter, K. D., Harley, M. D., Simmons, J. A., & Turner, I. L. (2019). CoastSat: A Google Earth Engine-enabled Python toolkit to extract shorelines from publicly available satellite imagery. *Environmental Modelling & Software*, *122*, 104528. https://doi.org/10.1016/j.envsoft.2019.104528

Voss, K. a, Famiglietti, J. S., Lo, M., Linage, C., Rodell, M., & Swenson, S. C. (2013). Groundwater depletion in the Middle East from GRACE with implications for transboundary water management in the Tigris-Euphrates-Western Iran region. *Water Resources Research*, *49*(2), 904–914. https://doi.org/10.1002/wrcr.20078

White, J. T., Hemmings, B., Fienen, M. N., & Knowling, M. J. (2021). Towards improved environmental modeling outcomes: Enabling low-cost access to high-dimensional, geostatistical-based decision-support analyses. *Environmental Modelling & Software*, *139*, 105022. https://doi.org/10.1016/j.envsoft.2021.105022

Yang, L., Driscol, J., Sarigai, S., Wu, Q., Chen, H., & Lippitt, C. D. (2022). Google Earth Engine and Artificial Intelligence (AI): A Comprehensive Review. *Remote Sensing*, *14*(14), 3253. https://doi.org/10.3390/rs14143253

Zhang, H., Xu, Y., & Kanyerere, T. (2020). A review of the managed aquifer recharge: Historical development, current situation and perspectives. *Physics and Chemistry of the Earth*, *118–119*. https://doi.org/10.1016/j.pce.2020.102887

Zomlot, Z., Verbeiren, B., Huysmans, M., & Batelaan, O. (2015). Spatial distribution of groundwater recharge and base flow: Assessment of controlling factors. *Journal of Hydrology: Regional Studies*, *4*, 349–368. https://doi.org/10.1016/j.ejrh.2015.07.005